Molecular Biology of the Cell
Vol. 21, 4089–4107, December 1, 2010

Assembly of Connexin43 into Gap Junctions Is Regulated Differentially by E-Cadherin and N-Cadherin in Rat Liver Epithelial Cells

Rajgopal Govindarajan,* Souvik Chakraborty,† Kristen E. Johnson,† Matthias M. Falk,‡ Margaret J. Wheelock,† Keith R. Johnson,† and Parmender P. Mehta†

†Department of Biochemistry and Molecular Biology, Eppley Institute for Research in Cancer and Allied Diseases, Eppley Cancer Center, University of Nebraska Medical Center, Omaha, NE 68198; and ‡Department of Biological Sciences, Lehigh University, Bethlehem, PA, 18015

Submitted May 7, 2010; Revised September 15, 2010; Accepted September 22, 2010
Monitoring Editor: Asma Nusrat

Cadherins have been thought to facilitate the assembly of connexins (Cxs) into gap junctions (GJs) by enhancing cell–cell contact, however the molecular mechanisms involved in this process have remained unexplored. We examined the assembly of GJs composed of Cx43 in isogenic clones derived from immortalized and nontransformed rat liver epithelial cells that expressed either epithelial cadherin (E-Cad), which curbs the malignant behavior of tumor cells, or neuronal cadherin (N-Cad), which augments the invasive and motile behavior of tumor cells. We found that N-cad expression attenuated the assembly of Cx43 into GJs, whereas E-Cad expression facilitated the assembly. The expression of N-Cad inhibited GJ assembly by causing endocytosis of Cx43 via a nonclathrin-dependent pathway. Knock down of N-Cad by ShRNA restored GJ assembly. When both cadherins were simultaneously expressed in the same cell type, GJ assembly and disassembly occurred concurrently. Our findings demonstrate that E-Cad and N-Cad have opposite effects on the assembly of Cx43 into GJs in rat liver epithelial cells. These findings imply that GJ assembly and disassembly are the down-stream targets of the signaling initiated by E-Cad and N-Cad, respectively, and may provide one possible explanation for the disparate role played by these cadherins in regulating cell motility and invasion during tumor progression and invasion.

INTRODUCTION

The cell–cell and cell–matrix adhesion molecules and their associated proteins often assemble into large macromolecular complexes, such as adherens junctions, desmosomes, tight junctions, and hemi-desmosomes and maintain the polarized and differentiated state of epithelial cells (Bryant and Mostov, 2008). Most cells in a polarized epithelium are also interconnected by another class of junctions, called GJs, which permit the direct passage of small molecules ($\leq$ 1 kDa) between adjoining cells (Goodenough and Paul, 2009). Gap junctions are ensembles of several cell–cell channels that are formed by a family of ~20 related proteins, called Cxs, which have been designated according to their molecular mass. A gap junctional cell–cell channel is formed when Cxs first oligomerize as hexamers to form a connexon, which, upon reaching the cell surface, docks with a connexon displayed by an adjacent cell (Segretain and Falk, 2004; Laird, 2006). Cell–cell communication mediated by gap junctional channels has been shown to regulate the proliferation and differentiation of epithelial cells and thus to fulfill a homeostatic role (Saez *et al*., 2003; Goodenough and Paul, 2009). Impaired, or loss of, Cx expression has been implicated in the pathogenesis of several forms of neoplasia as evidenced by in vitro and in vivo studies showing induction of cellular differentiation and attenuation of the malignant phenotype upon forced expression of Cxs in tumor cells and by gene knock out studies in transgenic mice (Wei *et al*., 2004; Crespin *et al*., 2009). Mutations in several Cx genes have been characterized in inherited diseases associated with aberrant cellular proliferation and differentiation (Laird, 2010).

In contrast to the well-established role of tight and adherens junctions, the role of GJs in initiating and maintaining the polarized and differentiated state of epithelial cells is not understood and remains yet to be explored. The importance of investigating this is underscored by the fact that loss of the polarized and differentiated state of epithelial cells is the hallmark of a variety of carcinomas as they progress from an indolent to an invasive state as well of epithelial to mesenchymal transformation (EMT) in which tumor cells become more migratory and motile (Thiery *et al*., 2009). It is thought that these changes are induced upon disruption of several

This article was published online ahead of print in *MBoC in Press* (http://www.molbiolcell.org/cgi/doi/10.1091/mbc.E10–05–0403) on September 29, 2010.

*Department of Pharmaceutical and Biomedical Sciences, University of Georgia, Athens, GA 30602.

Address correspondence to: Parmender P. Mehta (pmehta@unmc.edu).

Abbreviations used: Cx, connexin; GJ, gap junction; Cad, cadherin; EMT, epithelial mesenchymal transformation.

junctional complexes (Mosesson *et al*., 2008). Moreover, recent studies have shown that forced expression of Cxs partially reverses EMT-like characteristics acquired by breast cancer cells (McLachlan *et al*., 2006) and that maintenance of tight junctions may be dependent on the formation of GJs in some cell types (Kojima *et al*., 2007).

A first step toward elucidation of the role of GJs in maintaining the polarized and differentiated state of epithelial cells is to examine their assembly and disassembly upon loss or alteration of this state. Because bidirectional signaling between cadherins and Cxs has been implicated in the assembly of GJs (Musil *et al*., 1990; Jongen *et al*., 1991; Meyer *et al*., 1992; Hernandez-Blazquez *et al*., 2001; Wei *et al*., 2005), and because cadherins have been shown to play an important role in tumor progression and EMT (Wheelock and Johnson, 2003; Wheelock *et al*., 2008; Thiery *et al*., 2009), we explored the role of E-Cad, a cadherin expressed widely by epithelial cells, and N-Cad, a cadherin expressed by neuronal and mesenchymal cells (Tepass *et al*., 2000; Gumbiner, 2005), in controlling the assembly and disassembly of GJs. We chose these cadherins because they have been shown to affect the behavior of epithelial tumor cells in a diametrically opposed way, although both mediate cell–cell adhesion in cells in which they are normally expressed. For example, loss of, or dysfunctional, E-Cad mediated cell–cell adhesion facilitates the dissemination of tumor cells and confers upon them a more invasive state. On the other hand, it is the gain of N-Cad by the tumor cells that augments the dissemination of tumor cells and increases their migration and motility (Cavallaro and Christofori, 2004; Wheelock *et al*., 2008). Also, several studies have shown that one of the hallmarks of tumor progression and EMT is the gain of N-Cad expression by tumor cells, which may or may not be accompanied by the concomitant loss of E-Cad expression (Cavallaro and Christofori, 2004; Wheelock *et al*., 2008; Thiery *et al*., 2009).

Based on the well-documented role of Cxs in suppressing tumor formation and the fact that Cx expression and GJ assembly are compromised in advanced stages of carcinomas (Mehta *et al*., 1999; King and Lampe, 2004; Crespin *et al*., 2009), as well as prompted by studies that showed inhibition of GJ assembly by N-Cad (Wang and Rose, 1997), we reasoned that the two cadherins could have opposite effects on the assembly of GJs, with E-Cad facilitating and N-Cad inhibiting the assembly. To test this notion, we studied the assembly of GJs composed of Cx43 in isogenic clones derived from rat liver clone 9 (RL-CL9) cells that expressed either E-Cad or N-Cad. We show here that N-Cad expression attenuates GJ assembly by triggering endocytosis of Cx43 by a nonclathrin dependent pathway upon arrival at the cell surface, whereas knock down of N-Cad, or expression of E-Cad, facilitates the assembly. Our findings document that GJ assembly is one of the downstream targets of signaling initiated by these cadherins and may rationally explain some of the intriguing and at times contrasting roles of E-Cad and N-Cad in regulating cell adhesion, migration, and motility of tumor cells.

MATERIALS AND METHODS

Cell Culture

Immortalized and nontransformed rat liver clone 9 (RL-CL9) epithelial cells were purchased from ATCC and have been described earlier (Mehta *et al*., 1986; Mehta *et al*., 1992). Stock cultures were maintained by seeding 10^5 cells per 10-cm dish in DMEM (GIBCO, Grand Island, NY) supplemented with 5% defined fetal bovine serum (Hyclone, Salt Lake City, UT) in an atmosphere of 5% CO_2/95% air. Cells were passaged once a week and used between passages 3–12. New stock cultures were initiated every month from frozen vials. This schedule was strictly maintained. The retroviral packaging cell lines, Phoenix 293T, PA317, and PTi67 were grown as described previously (Mitra *et al*., 2006). RL-CL9 cells were infected with various recombinant retroviruses, and pooled cultures were grown and maintained in complete medium containing G418 (200 μg/ml), puromycin (2 μg/ml), and G418 plus puromycin (see retroviruses and retrovirus infection).

Isolation of Isogenic Subclones from RL-CL9 Cells Expressing E-Cadherin and N-Cadherin

One hundred RL-CL9 cells from passages 4 and 30 were seeded in 10-cm dishes in complete culture medium and allowed to grow into colonies. Between 63–100 clones from early and late passage cells were isolated using glass cylinders and expanded and frozen. Each clone was analyzed separately by Western blot and immunocytochemical analysis for the expression of E-Cad, N-Cad, Cx43 as well as for subcellular localization. Subclones that expressed only E-Cad and no detectable level of N-Cad were designated as RL-EΔN cells whereas subclones that expressed N-Cad and no detectable level of E-Cad were designated as RL-NΔE cells. Further characterization of these clones is described in Results.

Plasmids, Retroviral Vectors, and Other Recombinant DNA Constructs

We used the following retroviral vectors for our studies. 1. LXSN, LZRS-neo and LZRS-pac (control retroviruses). 2. LXSNCx32 harboring rat Cx32. 3. LXSNE-Cad (human), which was constructed by subcloning E-Cad into the EcoR1 and BamH1 sites of LXSN. 4. LZRS-E-Cad-Myc and LZRS-N-Cad-Myc expressing Myc-tagged human E-Cad and N-Cad. 5. ShN-Cad, ShP-Cad, and ShEGFP in pSuper.Retro.puro. The construction of these retroviral vectors has been described (Mehta *et al*., 1999; Nieman *et al*., 1999; Kim *et al*., 2000a; Govindarajan *et al*., 2002; Maeda *et al*., 2005; Maeda *et al*., 2006; Mitra *et al*., 2006; Shintani *et al*., 2008). GFP-tagged Rab5 and Rab7 and their constitutively active mutants, Rab5Q-L and Rab7Q-L, were kind gifts from Dr. Caplan. These retroviral vectors were used to produce recombinant retroviruses in HEK293T, PA317 and PTi67 amphotropic packaging cell lines as described (Mitra *et al*., 2006; Chakraborty *et al*., 2010). RL-CL9 cells were multiply (2–4 times) infected with various recombinant retroviruses and selected in either G418 (400 μg/ml) or puromycin (2 μg/ml) for 2–3 wk in complete medium. Pooled cultures from 1000–2000 colonies obtained from three to four dishes were expanded, frozen, and maintained in G418 (200 μg/ml) and in G418 and puromycin (2 μg/ml). Pooled polyclonal cultures were used within two to three passages for immunocytochemical and biochemical analyses.

Cell Surface Biotinylation Assay

Cells (2×10^5) were seeded in 6-cm dishes in 4 ml of complete medium and grown to confluence. Cell surface biotinylation was performed at 4°C by incubation with freshly prepared EZ-LinkSulfo-NHS-SS Biotin reagent (Pierce; Rockford, IL) at 0.5 mg/ml in phosphate buffered saline (PBS) supplemented with 1 mM $CaCl_2$ and 1 mM $MgCl_2$ (PBS-PLUS) for 1 h as described (VanSlyke and Musil, 2000; Chakraborty *et al*., 2010). The reaction was quenched with PBS-PLUS containing 20 mM glycine and cell lysis and affinity precipitation of biotinylated proteins were performed with 100 μg of total protein using 50 μl of streptavidin agarose beads (Pierce, Rockford, IL) on a rotator overnight at 4°C. The streptavidin-bound biotinylated proteins were eluted by incubating the beads for 30 min in 1× SDS loading buffer and resolved by SDS-PAGE followed by Western blotting. As an input, equal amount of total protein (10 μg) was also subjected to SDS-PAGE and Western blot analysis. To determine the kinetics of degradation of cell-surface associated Cx43, cells were biotinylated at 4°C as described above and, after washing and quenching biotin, were chased at 37°C for various times before affinity precipitation of the biotinylated proteins with streptavidin. The protein concentration was determined using BCA reagent (Pierce).

Detergent Extraction and Western Blot Analysis of Cx43 and Cx32

Cell lysis, detergent solubility assay with 1% Triton X-100 (TX-100), and Western blot analysis were performed as described (VanSlyke and Musil, 2000; Mitra *et al*., 2006; Chakraborty *et al*., 2010). Briefly, 5×10^5 RL-EΔN and RL-NΔE cells were seeded per 10-cm dish in 10 ml of complete medium and grown to confluence. Cells were then lysed in buffer SSK (10 mM Tris, 1 mM EGTA, 1 mM PMSF, 10 mM NaF, 10 mM NEM, 10 mM Na_2VO_4, 10 mM iodoacetamide, 0.5% TX-100, pH 7.4) supplemented with the protease inhibitor cocktail (Sigma, St. Louis, MO). To determine the detergent solubility of Cx43, the concentration of TX-100 was raised to 1% before ultracentrifugation at 100,000 × *g* for 60 min (35,000 rpm in analytical Beckman ultracentrifuge; Model 17–65 using a SW50.1 rotor). The detergent-insoluble pellets were dissolved in buffer C (70 mM Tris/HCl, pH 6.8, 8 M urea, 10 mM NEM, 10 mM iodoacetamide, 2.5% SDS, and 0.1 M DTT). After normalization based on cell number, the total, TX-100-soluble, and -insoluble fractions were mixed with 4× SDS-loading buffer to a final concentration of 1× and boiled at 100°C for 5 min (for Cx43) or incubated at room temperature for 1 h (for Cx32) before SDS-PAGE analysis.

Detergent (TX-100) Extraction of Cells In Situ

RL-EΔN and RL-NΔE cells were extracted in situ with 1% TX-100 essentially as described previously (Govindarajan *et al*., 2002; Chakraborty *et al*., 2010). In brief, 2.5×10^5 cells were seeded per well in six-well clusters containing glass cover slips and were grown for 2–3 d when they attained confluence. The cells were rinsed once in PBS and then incubated in isotonic medium (30 mM HEPES, pH 7.2; 140 mM NaCl; 1 mM $CaCl_2$, 1 mM $MgCl_2$) supplemented with the protease inhibitor cocktail (Sigma, MO) for 45 min at 4°C in the presence and absence of 1% TX-100. The dishes were swirled gently and intermittently. After incubation, cells were fixed and immunostained with appropriate primary and secondary antibodies as described below. The detergent-solubility of Cxs in single RL-EΔN and RL-NΔE cells was examined 24–36 h after seeding between 1 and 2×10^3 cells per well in six-well clusters. Under these conditions between 50 and 60% of seeded cells remained single and well-spread.

Antibodies and Immunostaining

Rabbit polyclonal and mouse monoclonal antibodies against Cx43 and Cx32 have been described earlier (Mehta *et al*., 1999). Rabbit anti-EEA-1 (PA1–063) was obtained from Affinity BioReagents (Golden, CO). Rabbit anti–caveolin-1 and anti–caveolin-2 were purchased from BD Transduction laboratories (San Jose, CA). Mouse anti-occludin (clone OC-3F10) was from Zymed Laboratories (South San Francisco, CA). Rabbit anti–α-catenin, rabbit anti–β-catenin, rabbit anti-Cx32 (loop and tail), and mouse anti–β-actin (clone C-15) antibodies were from Sigma (St. Louis, MO). Mouse anti-ZO1 (610967) and mouse anti-GM130 (610822) antibodies were obtained from BD Transduction laboratories (San Jose, CA). Mouse anti-clathrin heavy chain (MAI-065) was purchased from Affinity Bioreagents (Rockford, IL). Mouse anti-N-Cad, mouse anti-E-Cad, mouse anti–α-catenin, and mouse anti–β-catenin antibodies have been previously described (Maeda *et al*., 2005; Mitra *et al*., 2006; Shintani *et al*., 2008; Chakraborty *et al*., 2010). We also used rabbit anti–E-Cad antibody for immunostaining rat E-Cad. The production of this antibody has been described (Wheelock *et al*., 1987). Alexa-488 and Alexa-594 phalloidins as well as Alexa-488 and Alexa-594 conjugated cholera toxin, transferrin, and EGF were purchased from Invitrogen (Molecular Probes/Invitrogen, Eugene, OR).

RL-EΔN and RL-NΔE cells (see Results), seeded in six-well clusters at a density of 2.5×10^4/well and allowed to grow to confluence, were immunostained at room temperature with various antibodies at appropriately calibrated dilutions after fixing with 2% para-formaldehyde for 15 min as described previously (Mitra *et al*., 2006; Chakraborty *et al*., 2010). Secondary antibodies (rabbit or mouse) conjugated with Alexa-488 and Alexa-594 were used as appropriate. Images of immunostained cells were acquired with a Leica DMRIE microscope (Leica Microsystems, Wetzler, Germany) equipped with Hamamatsu ORCA-ER CCD camera (Hamamatsu City, Japan). For colocalization studies, serial *z* sections (0.5 μm) were collected and analyzed after iterative deconvolution using image-processing software (Volocity; Improvision, Lexington, MA). SlowFade antifade (Molecular Probes/Invitrogen) was used to mount cells on glass slides.

Cell Growth on Transwell Filters

RL-CL9, RL-EΔN, and RL-NΔE cells (2×10^4) were plated onto 12-mm transwell filters (pore size, 0.4 μm; Corning Life Sciences, MA) and grown for 7–21 d as described (Chakraborty *et al*., 2010). Medium of the upper and lower filter chambers was changed on alternate days. The immnunocytochemical analyses were performed directly on filters, after which the filters were cut with a sharp scalpel and mounted on glass slides with their cell side facing up. A drop of SlowFade antifade was placed on top followed by a glass coverslip, which was pressed gently using a 50 gm weight overnight. The edges were sealed with nail polish.

Cell Aggregation Assay

The hanging drop suspension culture method was used to test aggregation of RL-EΔN and RL-NΔE cells as described (Chakraborty *et al*., 2010). After harvesting with trypsin/EDTA, cells were resuspended at 2.5×10^5 cells per ml in complete culture medium and a 20-μl drop of medium containing 5×10^3 cells was suspended as a hanging drop from the lid of a 10 cm^2 Petri dish (40 hanging drops per lid) filled with PBS to prevent drying of the drops. The cells were then allowed to aggregate in a humidified 5% CO_2 incubator at 37°C for 16–20 h after which cells and aggregates were triturated five times with a standard 200 μl pipette tip to disperse loosely associated cells and a coverslip was placed gently on top of the cells. The cells were visualized by phase-contrast light microscopy at ×5 magnification and images captured using a CCD camera (Retiga 2000R, FAST 1394) mounted on a Leica DMRIE2 microscope with the aid of Volocity software (Improvision, Lexington, MA). For quantifying the size, the outline of each aggregate was drawn using an ROI tool and the area of each aggregate was measured. All images were analyzed at the same magnification and the area was recorded as "relative units" for each aggregate. The average area of the aggregates was considered as a measure of aggregate formation.

Cell Migration Assay

RL-EΔN and RL-NΔE cells were seeded on LabTek two-well chamber slides and allowed to grow to confluence. Confluent monolayers of cells were wounded by manually scratching with a pipette tip. We chose scratch areas of equal width for these assays. After marking the positions of the wounds in the X-Y plane, cells were imaged every 30 min at 37°C in an atmosphere of 5% CO_2/95% air for 24 h in a live cell imaging chamber mounted on an Olympus IX81 motorized inverted microscope (Olympus America Inc; Center Valley, PA). The microscope was controlled by IX2-UCB U-HSTR2 motorized system with a focus drift compensatory device IX1-ZDC. Images were captured using a Hamamatsu ORCA ER2 CCD camera and processed by imaging software Slidebook version 5.0 (Intelligent Imaging Innovations, Denver, CO).

Gap Junctional Communication Assays

Gap junctional communication was measured by microinjecting fluorescent tracers, Alexa Fluor 488 (MW 570 Da; A-10436) and Alexa Fluor 594 (MW 760 Da; A-10438), and by scrape loading as described (Govindarajan *et al*., 2002; Chakraborty *et al*., 2010). Fluorescent tracers were microinjected with an Eppendorf InjectMan and FemtoJet microinjection systems (Models 5271 and 5242, Brinkmann Instrument, Westbury, NY) mounted on a Leica DMIRE2 microscope. The images of microinjected cells were captured using a CCD camera (Retiga 2000R, FAST 1394) with the aid of Volocity software (Improvision, Lexington, MA) one and five minutes after microinjection for RL-EΔN and RL-NΔE cells, respectively, and the number of fluorescent cells, excluding the microinjected one, was counted from the captured images that were stored as TIFF files as described previously (Govindarajan *et al*., 2002; Chakraborty *et al*., 2010).

Cells were scrape-loaded as described (Govindarajan *et al*., 2002; Chakraborty *et al*., 2010). Briefly, RL-EΔN and RL-NΔE cells were seeded in six-well clusters at a density of 2.5×10^4/well and allowed to grow to confluence. Cell culture medium from freshly confluent cells was removed and replaced with 1 ml of medium containing rhodamine-conjugated fluorescent dextrans (10 kDa, 1 mg/ml; fixable) and Lucifer yellow (0.5%). Cells were scrape-loaded using a sterile scalpel by two longitudinal scratches and incubated for one minute at room temperature. Cells were washed quickly two to three times with warm PBS containing calcium and magnesium and returned to the incubator for five minutes, after which the medium was removed, cells were washed two times with PBS and fixed with 3.7% buffered Formalin at room temperature. The autofluorescence of cells was quenched with 0.1 M glycine and after washing once with PBS, the cover slips were mounted on glass slides in a droplet of SlowFade. Images of the scrape-loaded cells were captured as described above.

Treatments

Stock solutions of brefeldin (BIOMOL) and monensin (Calbiochem) were prepared in ethanol at 10 mM and stored at −80°C in small aliquots. Stock solution of chlorpromazine (BIOMOL) was prepared at 50 mg/ml in ethanol and those of filipin and methyl-β-cyclodextrin were prepared in cell culture medium at 20 mM each and stored frozen at −80°C for up to 1 mo. All solutions were appropriately diluted in the cell culture medium at the time of treatment.

RESULTS

Characteristics of Rat Liver Clone 9 (RL-CL9) Cells

We used an immortalized, nontransformed rat epithelial cell line, called RL-CL9, to examine GJ assembly and disassembly (Mehta *et al*., 1986; Mehta *et al*., 1992). RL-CL9 cells have a typical epithelial morphology (Figure S-1A) and express adherens junction–associated proteins E-Cad and α- and β-catenins, and tight junction associated proteins, occludin and ZO-1; moreover, these cells form cortical actin bundles and form GJs composed of Cx43 (Figure 1A). Furthermore, when grown on transwell filters, these cells grow as a monolayer, continue to express Cx43 and ZO-1 (Figure 1B), and acquire a partially polarized state as assessed by increased height of these cells and apical distribution of Na-K ATPase (not shown). Finally, these cells express both mesenchymal markers, such as vimentin, and epithelial markers, such as cytokeratin 8 (data not shown).

Altered Cadherin Expression and Gap Junction Assembly

We fortuitously observed that upon serial propagation of RL-CL9 cells from passage 4 to greater than passage 20, a population of cells emerged that began to lose typical cob-

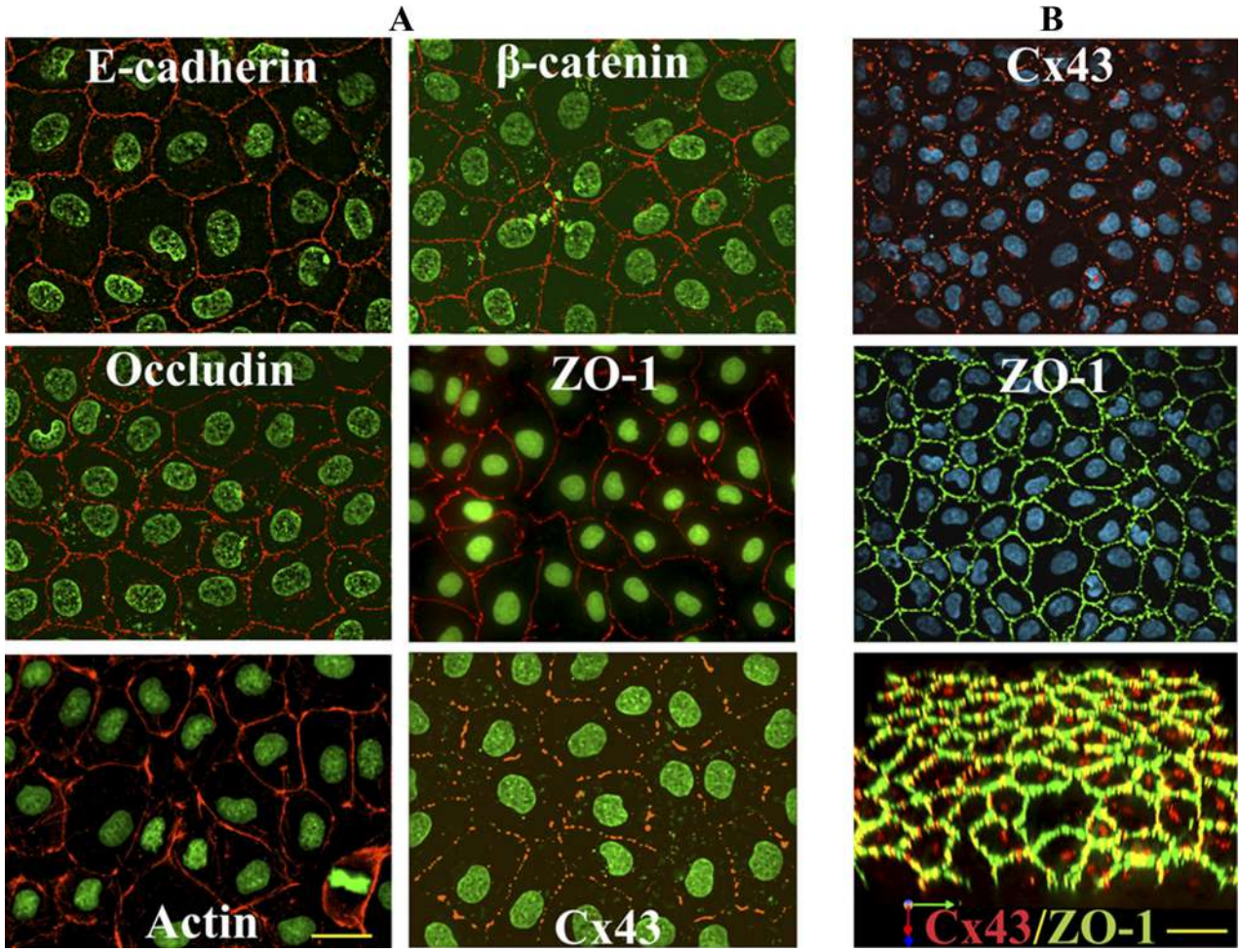

Figure 1. Expression of cell junction–associated proteins and Cx43 in RL-CL9 cells. (A) RL-CL9 cells, seeded in six-well clusters on glass coverslips, were immunostained for E-Cad and β-catenin, occludin and ZO-1, and actin and Cx43. Note robust expression of these proteins at cell–cell contact areas. (B) RL-CL9 cells were grown for 21 d on transwell filters and immunostained for Cx43 and ZO-1. Note that these cells form a uniform monolayer and continue to express Cx43 and ZO-1 robustly. Bottom image in B is the three-dimensional merged image of the top two images, which was volume rendered using Volocity. Nuclei (Green) were stained with DAPI. Bar = 20 μm in A and 10 μm in B.

blestone-like epithelial morphology (Figure S-1, top row). Moreover, immunocytochemical analysis showed that this population of cells began to express N-Cad (Figure S-1, middle row, left panel) in addition to E-Cad (Figure S-1, bottom row, middle panel). Furthermore, in this population of cells Cx43 was not assembled into GJs and was retained in the cytoplasm (Figure S-1, middle row). In addition, E-Cad expression at the areas of cell–cell contact of these cells appeared to be less robust and at times discontinuous (Figure S-1, bottom row, arrows). On systematic examination, we found that serial propagation of early passage RL-CL9 cells for 4–6 mo was gradually accompanied by an increase in the expression level of N-Cad (Figure S-2A, lower panels; Figure S-2C, blots) and vimentin (Figure S-2B, upper panels; Figure S-2C, blot), an increase in the proportion of cells in which actin was organized into stress fibers (Figure S-2B, bottom panels), and an increase in the proportion of cells in which Cx43 remained intracellular and failed to form GJs (not shown). Moreover, the expression level of E-Cad was not significantly altered (Figure S-2C), although some E-Cad began to accumulate in the cytoplasm (Figure S-2A, upper panels).

Gap Junction Assembly in E-Cadherin and N-Cadherin Expressing RL-CL9 Isogenic Subclones

To test whether gain of N-Cad expression was associated with the loss of GJ forming ability, we isolated between 63 and 92 clones from early and late passage RL-CL9 cells and examined the expression level and localization of Cx43, E-Cad, and N-Cad by immunocytochemical and Western blot analyses in each clone. We found that 70% of clones isolated from early passage (passage 4) RL-CL9 cells expressed only E-Cad and no detectable level of N-Cad, whereas 79% of clones isolated from late passage (passage 20) cells expressed only N-Cad and no detectable levels of E-Cad (Table S-1). Moreover, as assessed immunocytochemically, 61% of clones isolated from early passage RL-CL9 cells formed GJs whereas only 25% of clones isolated from late passage cells formed GJs (Table S-1). Furthermore, in clones in which both N-Cad and E-Cad were expressed to varying level, a fraction of Cx43 remained intracellular whereas a fraction was assembled into GJs (data not shown). For further study, we selected two E-Cad expressing clones lacking N-Cad expression, designated as RL-EΔN, and two

N-Cad expressing clones lacking E-Cad expression, designated as RL-NΔE, from early passage RL-CL9 cells to minimize the phenotypic and epigenetic changes that might have ensued upon serial propagation of early passage cells in vitro and which might have occurred in late passage RL-CL9 cells. Qualitatively similar data were obtained with both clones selected from each category and data from only one representative clone are shown in subsequent studies.

Gap Junction Assembly and Function in RL-EΔN and RL-NΔE Cells

As assessed by Western blot analysis, RL-EΔN cells expressed only E-Cad and no N-Cad, whereas RL-NΔE cells expressed only N-Cad and no E-Cad; moreover, the expression level of Cx43, α- and β-catenins, occludin and ZO-1, and cytokeratin 8 and vimentin was not significantly different (Figure 2, A and B). In RL-EΔN cells, Cx43 was assembled into GJs, whereas in RL-NΔE cells it was predominantly intracellular as discrete puncta although small puncta, which were barely detectable immunocytochemically, were also observed at cell–cell contact regions (Figure 2 B). Although no discernible difference in the expression level of actin was observed between RL-EΔN and RL-NΔE cells, actin was organized into cortical bundles in RL-EΔN cells whereas it was organized into more stress fibers in RL-NΔE cells as was observed in early passage and late passage RL-CL9 cells (data not shown, but see Figure 1 and Figure S-2B). Moreover, as was observed in early passage RL-CL9 cells, when grown on transwell filters, RL-EΔN cells grew as a monolayer, became columnar, and expressed ZO-1 robustly at the areas of cell–cell contact (Figure 2C, top row), whereas RL-NΔE cells formed a monolayer in which cell borders seemed to partially overlap. Furthermore, the pattern of localization of ZO-1 at areas of cell–cell contact was

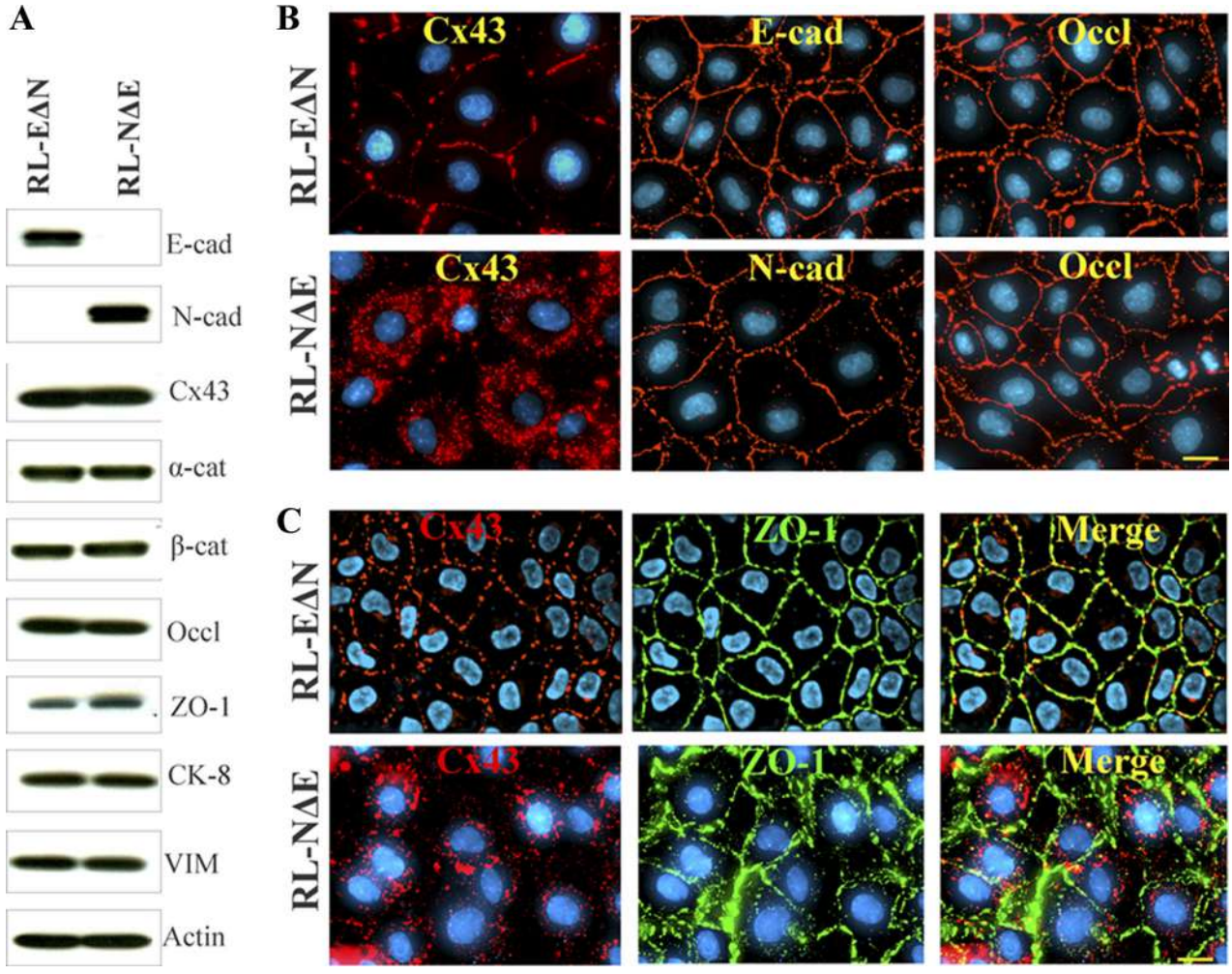

Figure 2. Localization and expression of Cx43, adherens and tight junction proteins, and cytoskeletal proteins in RL-EΔN and RL-NΔE cells. (A) Western blot analysis of the expression level of E-Cad (E-cad) and N-Cad (N-cad), Cx43, α- and β-catenins, occludin and ZO-1, cytokeratin 8 and vimentin and actin. Note that RL-EΔN cells express only E-Cad, but no detectable level of N-Cad, whereas RL-NΔE cells express only N-Cad but no E-Cad. Note also that the expression level of Cx43 and other proteins is not discernibly different in the two cell lines. (B) RL-EΔN and RL-NΔE cells were seeded on glass coverslips and immunostained for Cx43, E-Cad (E-cad), N-Cad (N-cad), and occludin (Occl). Note that Cx43 is assembled into GJs in RL-EΔN cells, whereas it remains intracellular as vesicular puncta in RL-NΔE cells. Note also that E-Cad, N-Cad, and occludin are localized at the areas of cell–cell contact in both cell types. (C) RL-EΔN and RL-NΔE cells were seeded on transwell filters for 5 d and immunostained for Cx43 and ZO-1. Note a more robust expression of ZO-1 at cell–cell contact areas in RL-EΔN cells compared with RL-NΔE cells. Note also partial overlap of cell boundaries in RL-NΔE cells as well as GJ like punctate structures. Nuclei (Blue) were stained with DAPI. Bar = 10 μm in B and 15 μm in C.

discontinuous and diffuse (Figure 2C, bottom row). In addition, although Cx43 appeared to have formed GJ like puncta due to partial overlap of the cell peripheries of the adjacent cells, such puncta were rarely observed at the areas of cell–cell contact upon careful examination (Figure 2C, bottom row). Compared with RL-EΔN cells which became columnar and could be maintained as a monolayer on filters for 2–3 mo, RL-NΔE cells became moribund and died within 10 d after attaining confluence. To corroborate the immunocytochemical data, we measured the junctional transfer of fluorescent tracer, Lucifer Yellow (MW 443), by scrape-loading (Figure 3A), and of Alexa 488 (MW 570) and Alexa 594 (MW 760), by microinjection (Figure 3B), in cells grown on glass cover slips and transwell filters. We found that RL-EΔN cells communicated extensively whereas RL-NΔE cells did not communicate either on plastic or on transwell filters (Figure 3 and Table 1).

Because in contrast to RL-NΔE cells, Cx43 was assembled into GJs in RL-EΔN cells, we also investigated whether cell–cell adhesion mediated by E-Cad and N-Cad remained functional in both cell types. A hanging drop assay, which measures the rate and strength of cell–cell adhesion based on the size of cell aggregates formed over time as well as the resistance of the formed aggregates to a shearing force was used (Kim *et al*., 2000b). As shown in Table S-2 both RL-EΔN and RL-NΔE cells aggregated efficiently as assessed by the mean area of the aggregates. We also found that RL-EΔN and RL-NΔE cells failed to invade in a standard Matrigel invasion assay (data not shown). Standard scratch (wound) assays were performed to determine whether RL-NΔE cells were more motile compared with RL-EΔN cells. Live cell imaging of the scratches of equal width in three independent experiments showed that wounds were filled within 14 ± 2 h in RL-NΔE cells whereas 22 ± 2 h were required to fill the wounds in RL-EΔN cells (Figure S-3). The mean (± SE) rate of migration was significantly faster in RL-NΔE cells as compared with RL-EΔN cells ($p = 0.04$).

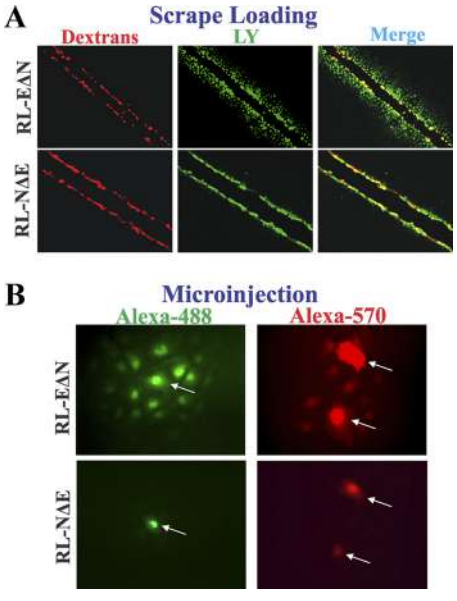

Figure 3. Gap junctional communication in RL-EΔN and RL-NΔE cells. (A) Cells were grown on glass coverslips and scrape-loaded with Lucifer Yellow and Alexa-594 conjugated dextrans. (B) Cells were microinjected with the indicated tracers as described in Materials and Methods. Note that in RL-EΔN cells, Lucifer Yellow has transferred from scrape-loaded (red) cells to neighboring cells, whereas no transfer is observed in RL-NΔE cells. Note also that the transfer of Alexa-488 and Alexa-570 from microinjected cells (indicated by arrows) to neighboring cells is observed only in RL-EΔN cells.

Table 1. Junctional communication of various fluorescent tracers in RL-EΔN and RL-NΔE cells*

Tracer	Exp. #	RL-EΔN	RL-NΔE	RL-NΔE (on filters)
Lucifer Yellow	1	24 ± 4† (20)‡	0 ± 0 (32)	0 ± 0 (21)
	2	22 ± 4 (20)	0 ± 0 (40)	0 ± 0 (20)
Alexa-488	1	13 ± 4 (20)	0 ± 0 (36)	0 ± 0 (33)
	2	12 ± 3 (20)	0 ± 0 (40)	0 ± 0 (44)
Alexa-594	1	4 ± 1 (20)	0 ± 0 (20)	0 ± 0 (29)
	2	6 ± 2 (20)	0 ± 0 (30)	0 ± 0 (38)

*Number of fluorescent cells 5 min after microinjection.

†Mean ± SE.

‡Number of mincroinjection trials. RL-EΔN and RL-NΔE cells were seeded in 6-cm Nunc dishes in replicate at a density of 2×10^5 cells per dish and allowed to grow to confluence for 4 days. Junctional communication was measured by microinjecting different fluorescent tracers as described in Materials and Methods.

Taken together, the data presented in Figures 2, 3, and S-3 and in Tables 1 and S-1 suggest that a switch in expression from E-Cad to N-Cad is associated with the attenuation of assembly and/or maintenance of GJs and their function, while the expression of E-Cad is associated with the facilitation of assembly and function. Moreover, these data also suggest that in RL-NΔE cells GJ assembly was not disrupted because of lack of cell–cell adhesion but by some other defect. Furthermore, these findings suggest that in RL-NΔE cells, N-Cad expression is more closely related with increased motility and with the loss of ability to grow and sustain a polarized monolayer on transwell filters than with invasion in Matrigel.

Detergent-Solubility of Cx43 in RL-EΔN and RL-NΔE Cells

To substantiate the immunocytochemical and functional data, and to elucidate the possible mechanism of attenuation of GJ assembly in RL-NΔE cells, we determined the assembly of Cx43 into GJs biochemically by Western blot analysis of total and Triton X (TX)-100-soluble and TX-insoluble cell fractions (VanSlyke and Musil, 2000). Intriguingly, a significant proportion of Cx43 was detected in detergent-insoluble fractions in both RL-EΔN and RL-NΔE cells (Figure 4A). Detergent solubility of live RL-NΔE and RL-EΔN cells by in situ extraction with 1% TX-100 showed that intracellular Cx43 puncta in RL-NΔE cells and intercellular gap junctional puncta in RL-EΔN cells were detergent-insoluble (Figure 4B). We also found that in RL-NΔE cells small intercellular puncta at areas of cell–cell contact, which were barely detectable immunocytochemically, remained detergent-resistant. The solubility of β-catenin, an adherens junction–associated protein, was not significantly affected in RL-EΔN and RL-NΔE cells (Figure 4B), whereas EEA1, a marker for the early endosomes, was lost upon in situ extraction (data not shown). These data suggest that a significant proportion of Cx43 in RL-NΔE cells is detergent-insoluble and that the detergent-insoluble fraction corresponds to discrete puncta that lie scattered throughout the cytoplasm, as well as to very small puncta that are seen at areas of cell–cell contact.

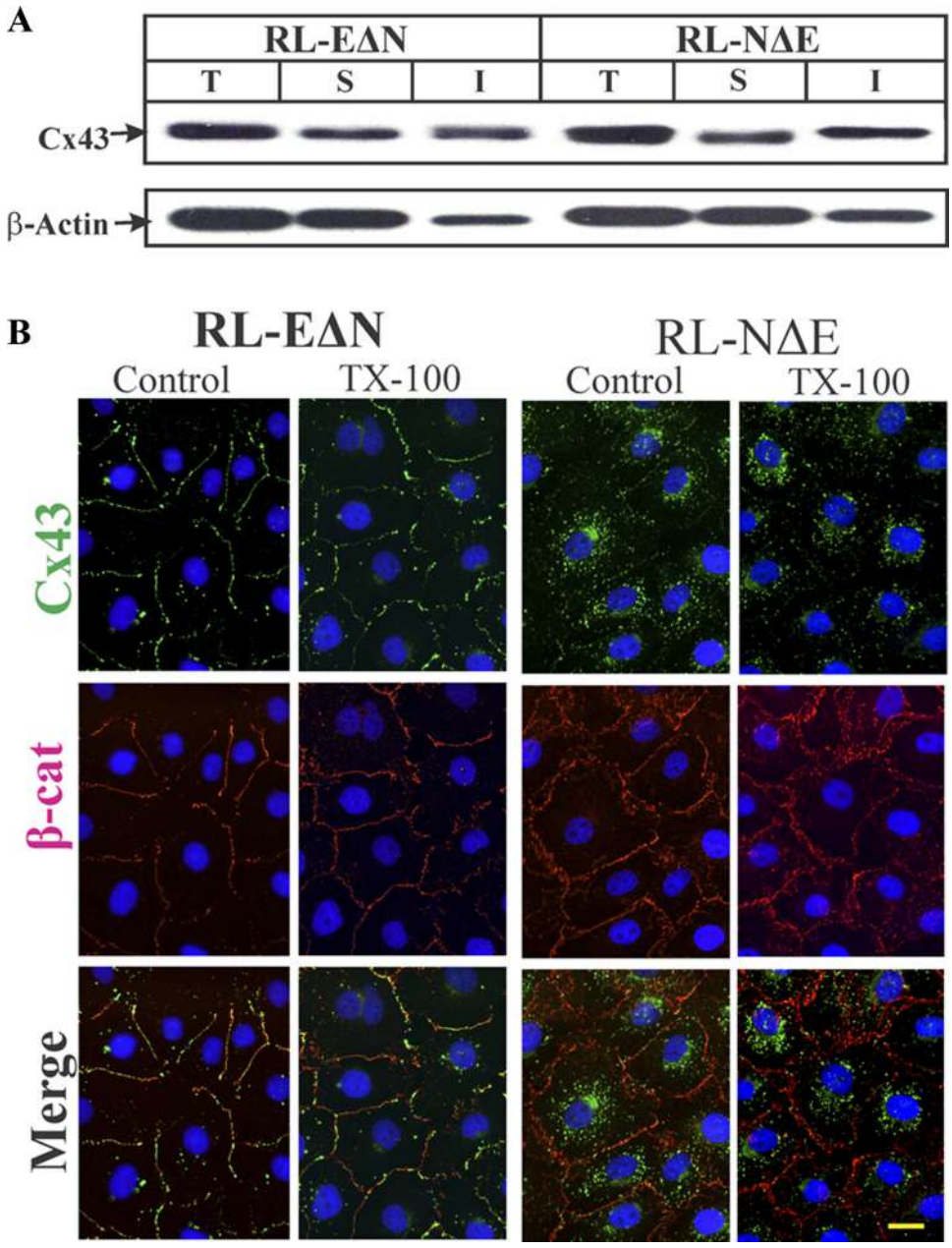

Figure 4. Detergent-solubility of Cx43 in RL-EΔN and RL-NΔE cells. (A) Total (T), TX-100-soluble (S), and TX–insoluble (I) fractions from cells were analyzed by Western blot analysis as described in Materials and Methods. The blots were stripped and reprobed with anti–β-actin antibody to verify equal loading. Note that Cx43 is detected in both detergent-soluble and detergent-insoluble fractions in both cell types. (B) Detergent solubility of Cx43 was examined in cells upon in situ extraction with 1% Triton X-100 at 4°C as described in Materials and Methods. Cells were immunostained for Cx43 (green) and β-catenin (red). Note that both junctional Cx43 in RL-EΔN cells and intracellular Cx43 in RL-NΔE cells were detergent-insoluble. Note also that the intensity of β-catenin at the areas of cell–cell contact is not significantly affected by the detergent treatment. Bar = 15 μm.

Opposing Effects of E-Cadherin and N-Cadherin on Gap Junction Formation

To explore further whether the expression of E-Cad and N-Cad affects GJ assembly in a diametrically opposed way, we undertook two complementary experimental approaches. First, we knocked down N-Cad in RL-NΔE cells using ShRNA. Second, we introduced human N-Cad in RL-EΔN cells and E-Cad in RL-NΔE cells. We used recombinant retroviruses to express and knock down cadherins. Also, for these experiments both N-Cad and E-Cad were myc-tagged to distinguish them from their endogenously expressed rat counterparts. An independent approach to knock down E-Cad using SiRNA was not successful as it failed to reduce the expression of E-Cad in RL-EΔN cells (unpublished). To minimize clonal heterogeneity, GJ assembly and cellular localization of Cx43 were examined in pooled polyclonal cultures within 1–3 passages after G418 or puromycin selection (see Materials and Methods). Figures 5 and 6 show the representative data from three independent sets of experiments and Table 2 provides the summary of the quantitative data.

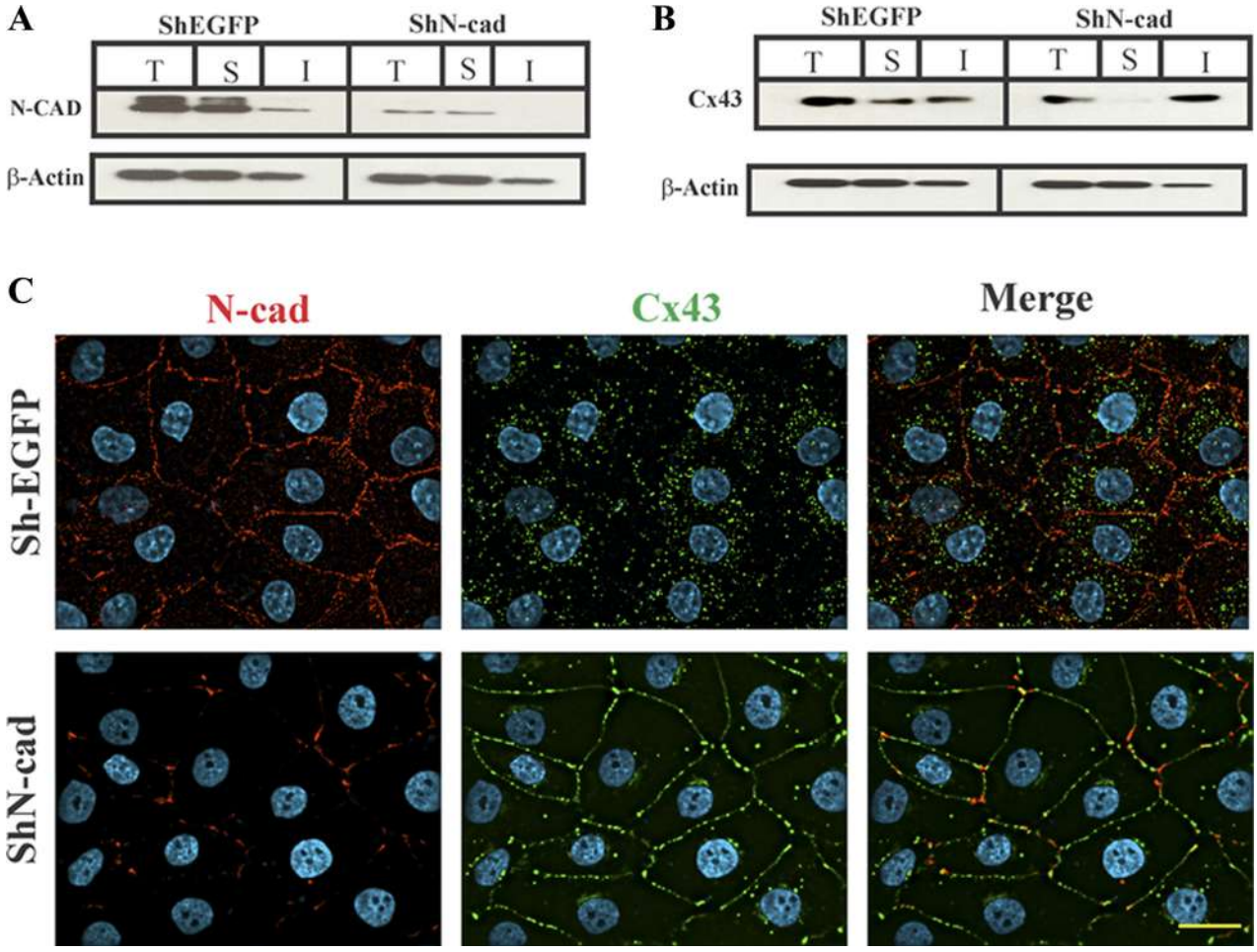

Figure 5. N-cadherin knockdown restores gap junction assembly in RL-NΔE cells. Cells were infected with ShEGFP and ShN-Cad and selected as described in Materials and Methods. Expression level of total (T), detergent-soluble (S), and detergent-insoluble (I) N-Cad (A) and Cx43 (B) were determined in cells infected with ShEGFP and ShN-Cad, respectively. Ten micrograms of total protein and normalized soluble and insoluble fractions were resolved on 12% SDS-PAGE and immunoblotted for Cx43 and N-Cad. The blots were reprobed with β-actin to verify equal loading. Note that the N-Cad expression level is significantly reduced in ShN-Cad infected pooled RL-NΔE polyclonal cultures (A), whereas the expression level of Cx43 (B) is not discernibly affected. Note also that knock down of N-Cad decreased the detergent soluble fraction, and increased the detergent-insoluble fraction, of Cx43. (C) Pooled polyclonal cultures of RL-NΔE cells infected with ShEGFP and ShN-Cad were immunostained for Cx43 and N-Cad. Note the reduced expression of N-Cad at areas of cell–cell contact and in the intracellular pool, the disappearance of intracellular Cx43, and GJ formation in cells infected with ShN-Cad but not with control retrovirus (ShEGFP). Bar = 15 μm.

As assessed immunocytochemically and by the densitometric scanning of Western blots, ShN-cad decreased the expression level of N-Cad by 80 ± 7% (n = 3) in RL-NΔE cells (Figure 5 A) with a concomitant decrease in the localization of N-Cad at the areas of cell–cell contact (Figure 5C, compare top left panel with the bottom left panel), decrease in the intracellular accumulation of Cx43 and an increase in GJ assembly (Figure 5C, compare top middle and right panels with the corresponding bottom panels). Knock down of N-Cad had no discernible effect on the expression level of Cx43 but decreased the detergent-soluble fraction without affecting the detergent-insoluble fraction significantly (Figure 5B). These effects were not observed when RL-NΔE cells were infected with ShEGFP (Figure 5, A and B, left panels) or ShP-Cad, an ShRNA directed against placental cadherin (not shown). Moreover, knock down of N-Cad neither induced E-Cad expression nor affected the expression level of ZO-1 and α- and β-catenins (data not shown).

In the next series of experiments, we introduced myc-tagged N-Cad in RL-EΔN cells and myc-tagged E-Cad in RL-NΔE cells. As assessed by immunocytochemical and Western blot analyses, E-Cad (Figure S-4A, bottom right panel; Figure S-4C) and N-Cad (Figure S-4B, bottom right panel; Figure S-4D) were expressed robustly and appropriately at the areas of cell–cell contact when introduced into RL-NΔE and RL-EΔN cells, respectively. As assessed by quantitative immunocytochemical analysis, we found that the expression of E-Cad in RL-NΔE cells induced GJ assembly and decreased intracellular Cx43 puncta (Figure 6A, Table 2), whereas the expression of N-Cad in RL-EΔN cells partially attenuated GJ assembly and caused intracellular accumulation of Cx43 (Figure 6B, Table 2). The expression of E-Cad in RL-NΔE cells had no discernable effect on the expression level of N-Cad and its localization (Figure S-4, A and C). Similarly, the expression of N-Cad had no detectable effect on the expression level of E-Cad and its localization in RL-NΔE cells (Figure S-4, B and D). Taken together, these data document that the presence of N-Cad at the cell surface is associated with the attenuation of GJ assembly, whereas the presence of E-Cad with the facilitation of the assembly.

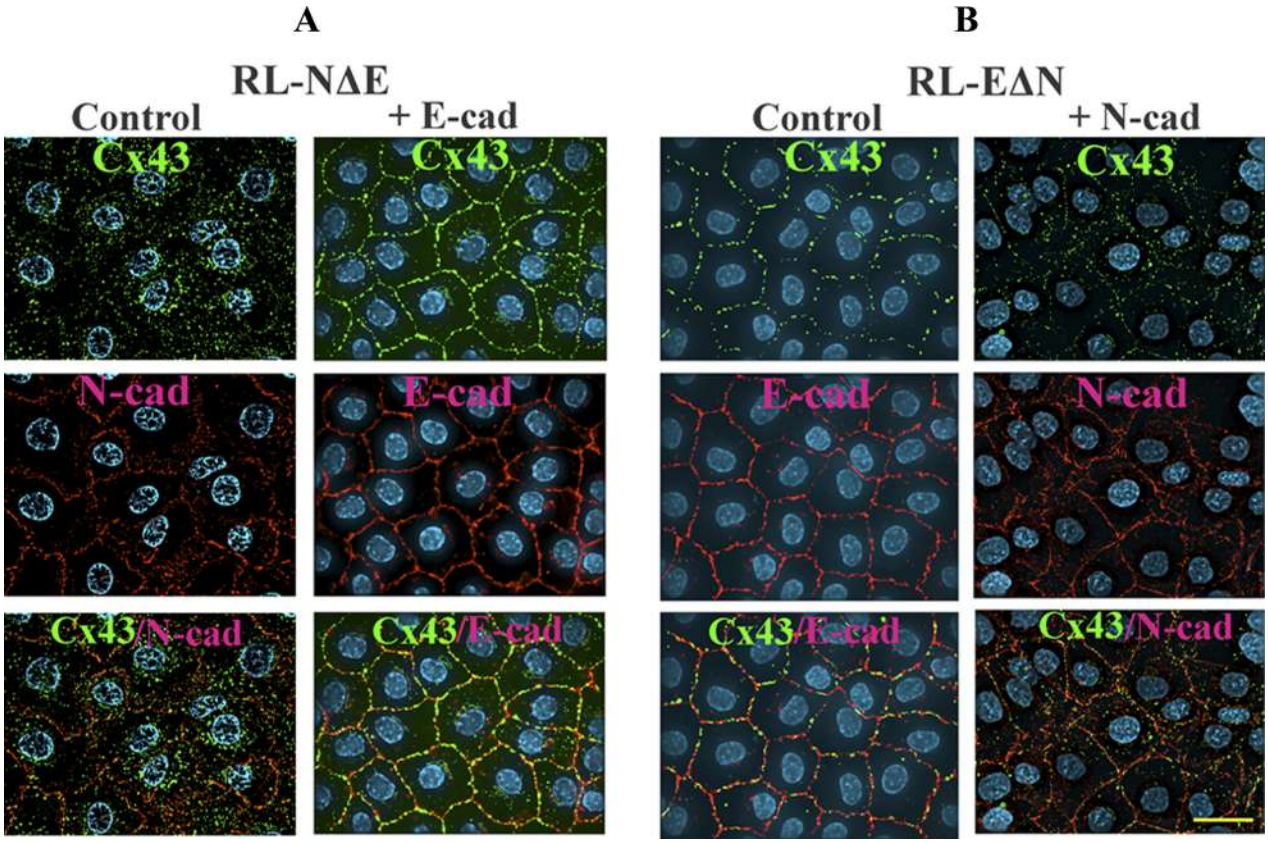

Figure 6. E-cadherin and N-cadherin have opposite effects on gap junction assembly. Myc-tagged N-Cad and E-Cad were introduced, respectively, into RL-EΔN and RL-NΔE cells as described in Materials and Methods. Pooled polyclonal cultures were immunostained for Cx43 (green) and either endogenous cadherin or Myc (red). Note that E-Cad expression (+E-Cad) in RL-NΔE cells restores GJ formation (A) and N-Cad expression (+N-Cad) in RL-EΔN cells partially disrupts GJ assembly (B) and induces intracellular accumulation of Cx43. Bar = 20 μm.

Cx43 Traffics Normally to Cell Surface in RL-NΔE and RL-EΔN Cells

We next explored the molecular basis of attenuation of GJ assembly and intracellular accumulation of Cx43 in RL-NΔE cells. Attenuation of GJ assembly and/or intracellular accumulation of Cx43 could be caused either by its impaired trafficking or by its endocytosis before GJ assembly upon arrival at the cell surface or by the endocytosis of minuscule GJs that remain very small. We used cell surface biotinylation to examine whether Cx43 trafficked normally to the cell surface in RL-NΔE and RL-EΔN cells. Figure 7A shows that Cx43 was biotinylated significantly in both RL-NΔE and RL-EΔN cells. To determine whether cell surface–associated Cx43 was degraded more rapidly in RL-NΔE cells compared with RL-EΔN cells, we determined the kinetics of its degradation after biotinylation. We found that cell surface biotinylated Cx43 degraded with a similar kinetics in both cell types (Figure 7, B–D). These findings suggest that intracellular accumulation of Cx43 in N-Cad expressing RL-NΔE cells is neither caused by impaired trafficking nor by altered kinetics of its degradation at the cell surface, but by some undefined mechanism that interferes with its assembly into GJs upon arrival at the cell surface resulting in its accumulation in intracellular vesicles or minuscule annular GJs.

Table 2. Effect of E-cadherin and N-cadherin expression on intracellular accumulation of connexin43 in RL-EΔN and RL-NΔE cells

Exp. #	RL-EΔN	RL-EΔN +N-Cadherin	RL-NΔE	RL-NΔE +E-Cadherin
1	5 ± 2	14 ± 6	24 ± 7	10 ± 4
2	7 ± 3	23 ± 7	33 ± 9	15 ± 5
3	4 ± 2	27 ± 9	37 ± 11	17 ± 11

N-cadherin and E-cadherin were introduced, respectively, into RL-EΔN and RL-NΔE cells (see Materials and Methods). Pooled polyclonal cultures were immunostained for Cx43 and E-cadherin and N-cadherin. Images were captured using 0.5-μm Z-steps and deconvolved. After merging all the deconvolved image stacks into a single plane, the number of intracellular puncta were counted in 10 randomly selected cells. E-cadherin or N-cadherin immunostaining was used to delineate cell boundaries. The mean number of puncta per cell ± SE was then calculated. Note that N-cadherin expression in RL-EΔN cells increased the number of intracellular puncta, whereas expression of E-cadherin in RL-NΔE cells had the opposite effect.

Cx43 Is Endocytosed by Nonclathrin-Mediated Pathway in RL-NΔE Cells

In RL-NΔE cells, Cx43 trafficked to the cell surface based on cell surface biotinylation, but failed to form functional GJs; moreover, a significant proportion of Cx43 remained detergent-insoluble as discrete intracellular puncta as assessed biochemically and immunocytochemically upon in situ ex-

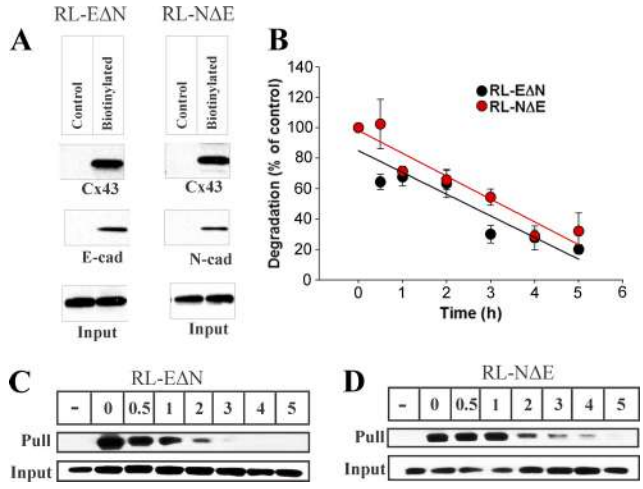

Figure 7. Cx43 traffics to cell surface in RL-EΔN and RL-NΔE cells. Confluent cultures of RL-EΔN and RL-NΔE cells (A) were biotinylated with sulfo-NHS-SS-biotin at 4°C, and biotinylated proteins from 100 μg of total cell lysate were detected by Streptavidin pull down followed by Western blotting for Cx43, E-Cad, and N-Cad (see Materials and Methods). In the lanes labeled Input, 10 μg of total protein was used and probed for Cx43. Note that in both RL-EΔN and RL-NΔE cells (A; labeled as Biotinylated), nearly the same amount of Cx43 was detected in the Streptavidin "Pull down" lanes. Note also that E-Cad and N-Cad were pulled down, respectively, only in RL-EΔN cells and RL-NΔE cells. A nonbiotinylated dish (labeled as Control) was used as a negative control. (B–D). Cell surface associated Cx43 degrades with similar kinetics in RL-EΔN and RL-NΔE cells. Cells were biotinylated at 4°C and were incubated for various times at 37°C before Streptavidin pull down and Western blotting as described in Materials and Methods. A nonbiotinylated dish was kept as a control (−). The blots were quantified after normalization of the input for each time point, and the values from three independent experiments were plotted graphically using Sigma plot as described in Materials and Methods. Note that cell surface associated biotinylated Cx43 degrades with similar kinetics in both RL-EΔN and RL-NΔE cells.

traction with 1% TX-100 (Figures 2–4). This raised the possibility that N-Cad expression attenuated GJ assembly either by triggering the endocytosis of connexons into detergent-insoluble puncta before their assembly into GJs or by triggering endocytosis of nascent, minuscule, and nonfunctional GJ plaques before their maturation into immunoctyochemically detectable, larger, and functional plaques (Jordan *et al.*, 2001; Piehl *et al.*, 2007; Falk *et al.*, 2009). Hence, we investigated whether Cx43 was endocytosed by a clathrin-mediated pathway or a nonclathrin-mediated pathway. We used chlorpromazine and hypertonic medium, which prevent the formation of clathrin coated pits, to block the clathrin-mediated pathway (Heuser and Anderson, 1989; Wang *et al.*, 1993), and filipin and methyl-β-cyclodextrin (MβCD), which impair the structure and function of sphingolipid-cholestrol-rich membrane microdomains (lipid rafts), to inhibit nonclathrin-mediated pathway (Subtil *et al.*, 1994; Orlandi and Fishman, 1998; Skretting *et al.*, 1999). Moreover, the specificity of these drugs in inhibiting each pathway was assessed by measuring the uptake of Alexa-594– or Alexa-488–labeled transferrin and cholera toxin, which are predominantly endocytosed by clathrin-mediated and nonclathrin-mediated pathways, respectively (Wang *et al.*, 1993; Subtil *et al.*, 1994; Orlandi and Fishman, 1998). For these experiments, RL-EΔN and RL-NΔE cells were treated with chlorpromazine (5 μg/ml), filipin (2.5 μg/ml), and MβCD (5 mM) for 2 h. These concentrations were determined based on several pilot experiments in which the dose and the duration of treatment were varied while the internalization of Alexa-488/594-labeled transferrin and cholera toxin was monitored microscopically. We found that both in RL-EΔN and RL-NΔE cells, chloropromazine and hypertonic media inhibited the uptake of only Alexa-488/594–labeled transferrin but did not affect the uptake of Alexa-488/594–labeled cholera toxin. Similarly, filipin and MβCD inhibited the uptake of only Alexa-488/594–labeled cholera toxin but did not affect the uptake of Alexa-488/594–labeled transferin (data not shown). Consistent with the effect of filipin and MβCD on the inhibition of uptake of cholera toxin, we found that they induced GJ assembly profoundly in RL-NΔE cells (Figure 8, bottom row, compare panel 1 with panels 3 and 4) but had no discernible effect on the assembly in RL-EΔN

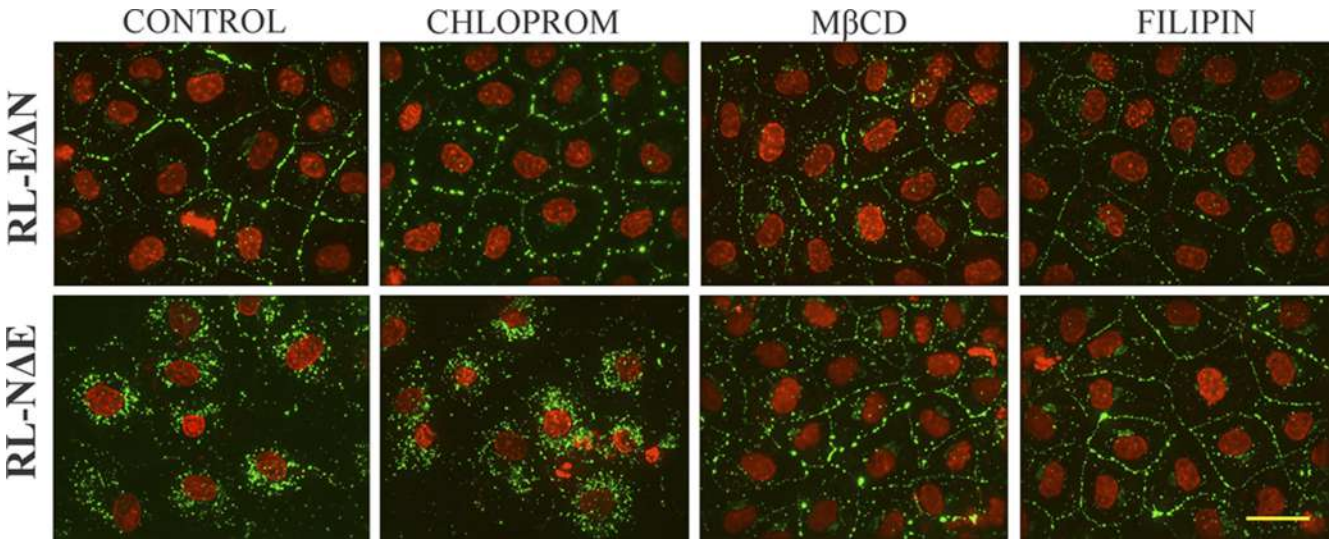

Figure 8. Inhibition of nonclathrin-dependent endocytosis restores gap junction assembly in RL-NΔE cells. RL-EΔN and RL-NΔE cells, seeded on glass cover slips in six-well clusters and allowed to grow to confluence, were treated with chlorpromazine (Chlorprom; 5 μg/ml), filipin (2.5 μg/ml), or methyl-β-cyclodextrin (MβCD, 5 mM) for 60 min. After washing and fixation, cells were immunostained for Cx43. Note that treatment with filipin and MβCD restored GJ assembly in RL-NΔE cells but had no significant effect on RL-EΔN cells. Bar = 20 μm.

cells (Figure 8, upper row, compare panel 1 with panels 3 and 4). On the other hand, chlorpromazine had no effect on GJ assembly in RL-NΔE cells (Figure 8, bottom row, compare panel 1 and 2) but appeared to decrease the preponderance of intracellular puncta in RL-EΔN cells as assessed visually (Figure 8, top row, compare panels 1 and 2). A rigorous quantitative analysis has to be performed to assess if chloropromazine enhanced GJ assembly in RL-EΔN cells. Similar data were obtained when RL-NΔE and RL-EΔN cells were treated with hypertonic medium (data not shown).

To further define the subcellular fate of intracellular puncta, we immunostained RL-NΔE cells with the markers specific for the endocytic pathway and examined whether they colocalized with Cx43. These analyses showed that Cx43 did not detectably colocalize with clathrin, a major structural component of clathrin-coated vesicles, with the early endosome marker, EEA-1, and with caveolin-2 (Figure 9) although some colocalization was observed with caveolin-1 both in the perinuclear region and at the cell surface consistent with what has been reported in earlier studies (Langlois *et al*., 2008). Because none of the commercially available antibodies recognized rat Rab5 and Rab7, we transiently expressed GFP-tagged, constitutively active, Rab5 and Rab7 in RL-NΔE cells and immunostained cells for Cx43 to examine whether it colocalized with these markers. We found that Cx43 did not colocalize with Rab5-GFP–positive vesicles, however some colocalization was observed with Rab7-GFP positive late endosomes (Figure S-5). Moreover, significant colocalization of Cx43 was observed with Lamp-1 (Figure S-5, bottom row), which is localized on lysosomes (Rohrer *et al*., 1996). Taken together, the above data suggest that in RL-NΔE cells connexons that arrive at the cell surface are either internalized before their docking and assembly into GJs or are assembled into minuscule GJs, which are endocytosed by nonclathrin dependent pathway into detergent-resistant puncta that eventually are targeted to lysosomes for degradation.

On the Origin of Detergent-Insoluble Intracellular Puncta in RL-EΔN and RL-NΔE Cells

In the next series of experiments, we explored the possible mechanisms by which detergent-resistant intracellular puncta might be generated. To test whether these puncta arose from the endocytosis of connexons that failed to dock with the adjacent connexons or from the formation of minuscule GJs, which acquired resistance to detergent extrac-

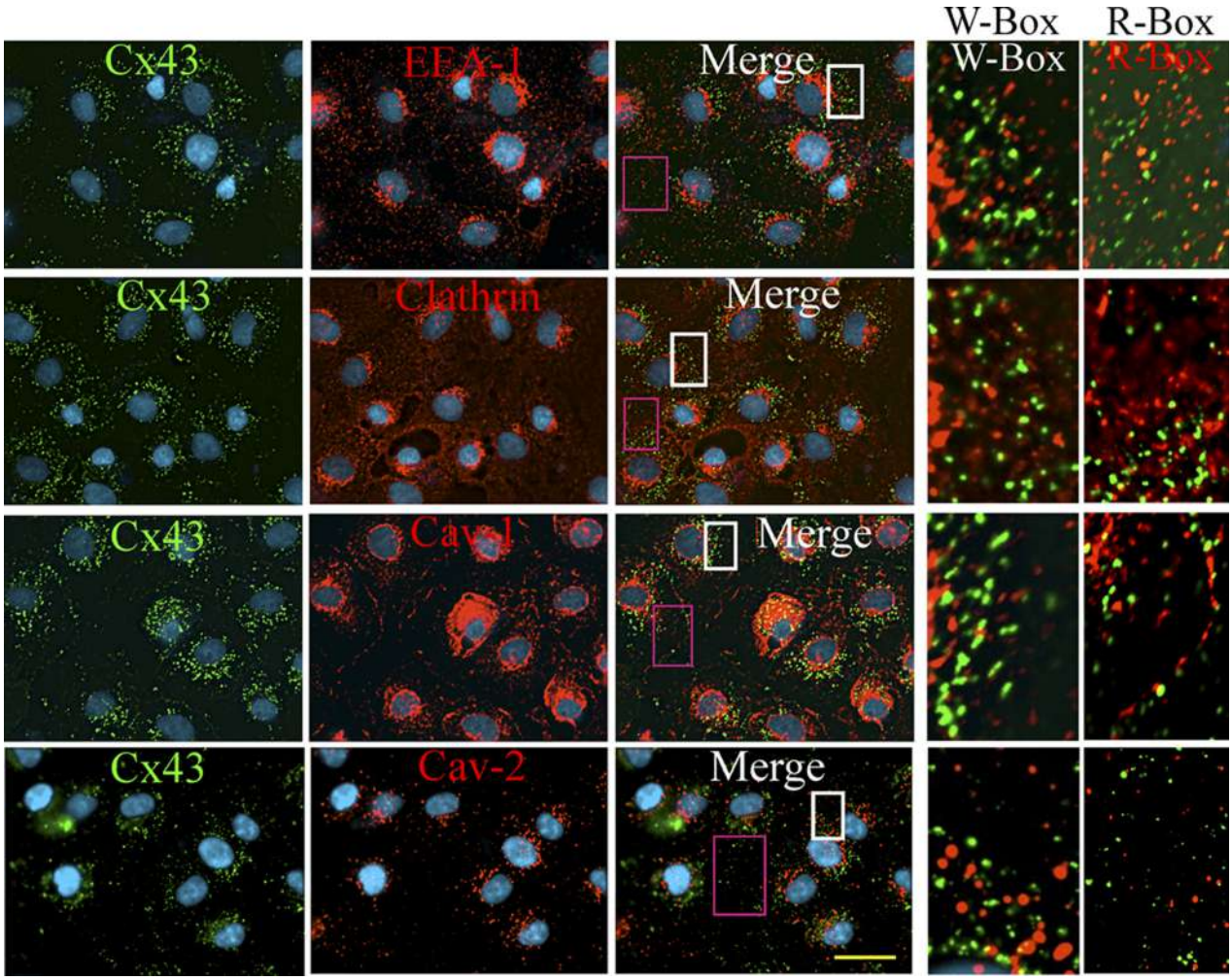

Figure 9. Cx43 does not colocalize with known endocytic markers in RL-NΔE cells. RL-NΔE cells, seeded as described in Figure 8 legend, were immunostained for Cx43 (green) and endocytic markers, EEA-1, clathrin, caveolin-1, and caveolin-2 (red). Note that Cx43 does not colocalize with any of these markers as shown in the enlarged images of the marked boxes on the right. W-Box = white box; R-Box = Red box. Bar = 20 μm.

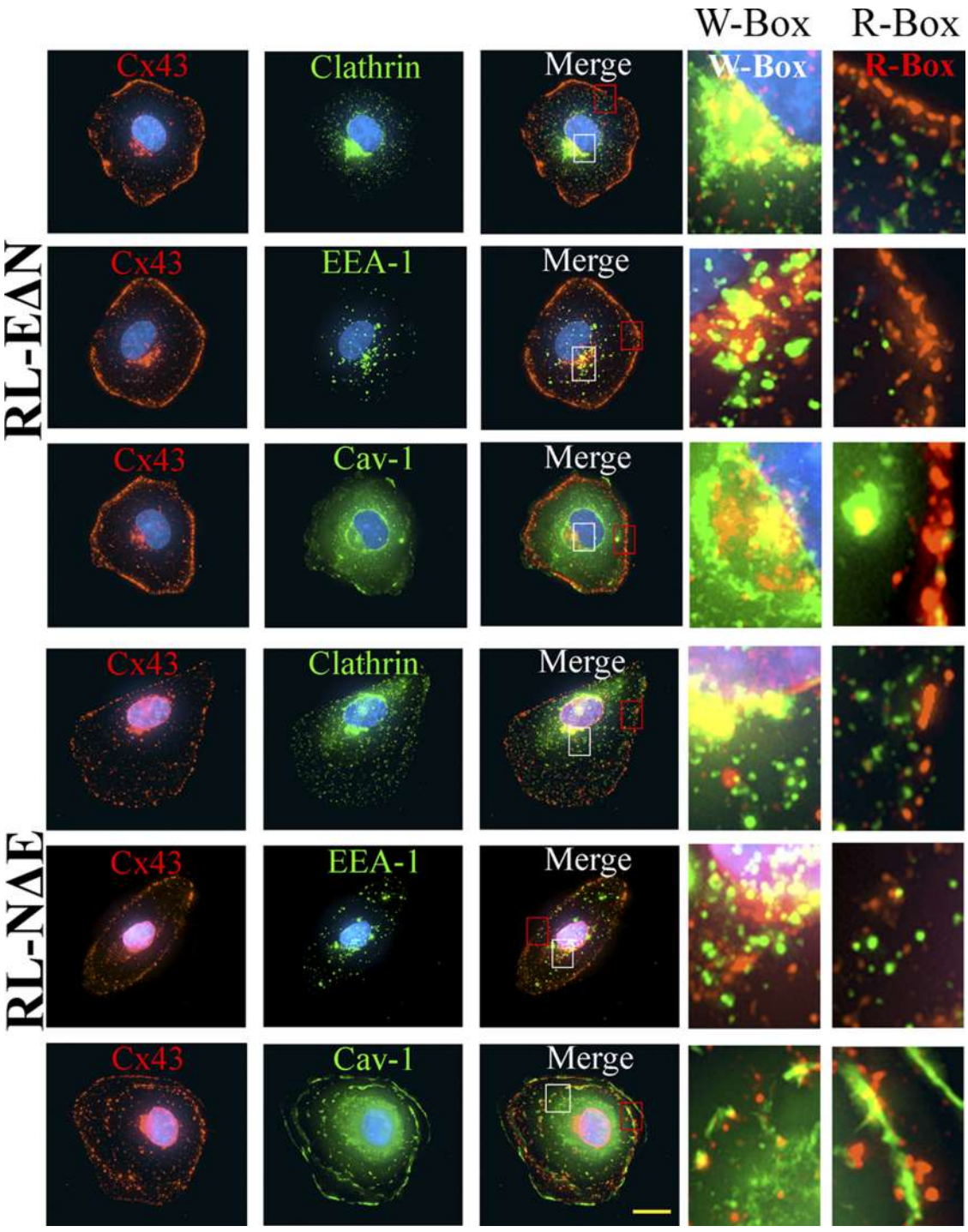

Figure 10. Cx43 is endocytosed into detergent-soluble puncta in RL-NΔE and RL-EΔN single cells. Between 1- 2 × 10^3 RL-EΔN and RL-NΔE cells were seeded on six-well clusters containing glass cover slips. The subcellular fate of Cx43 was examined in single cells upon in situ extraction with 1% Triton X-100 at 4°C as described in Materials and Methods. Cells were immunostained for Cx43 (green) and clathrin, EEA-1 and caveolin-1 (red). Enlarged images marked by the white boxes (W-box) and red boxes (R-box) are shown on the right. Note that significant colocalization with all the markers is observed in the perinuclear regions in both cell types, while partial localization to a variable extent is observed in the cell peripheries. All, punctuate and nonpunctate, immunostaining was lost upon detergent extraction (not shown). Bar = 7 μm.

tion, as has been observed during the formation of adherens junctions (Adams *et al.*, 1996), we examined the subcellular fate of intracellular puncta in single RL-NΔE and RL-EΔN cells 24–36 h after seeding and determined their detergent solubility upon in situ extraction with 1% TX-100 in 3 independent experiments. We rationalized that given the short half-life of Cx43 (2–5 h), intracellular puncta in single cells plausibly represent endocytosed undocked connexons that trafficked to the cell surface or vesicles along the secretory pathway. We found that in RL-NΔE and RL-EΔN single

cells, Cx43 was localized as discrete puncta both at the cell periphery and in the cytoplasm; moreover, as shown in representative images in Figure 10, these puncta colocalized with clathrin, EEA-1 and Cav-1 albeit to a variable extent. The extent of colocalization appeared to be more robust at the perinuclear region as compared with cell periphery. However, we found that in contrast to what was observed in confluent cells, all puncta—both intracellular and at the cell periphery—were lost upon in situ extraction with 1% TX-100 as assessed immunocytochemically (data not shown).

To rule out the possibility that the detergent-resistant puncta arose during the transit of Cx43 along the secretory pathway, we blocked ER to Golgi transport with brefeldin (Klausner *et al*., 1992; Chardin and McCormick, 1999) and *cis*-Golgi to *medial*-Golgi transport with monensin (Tartakoff, 1983). For these experiments, confluent RL-NΔE and RL-EΔN cells were treated with brefeldin (10 μM) and monesin (10 μM) for 30 min to 4 h and immunostained for Cx43 and GM130, a *cis*-Golgi resident protein (Marra *et al*., 2007). We found that in RL-NΔE cells, treatment with brefeldin for 1–4 h disrupted Golgi structure but did not diminish the number of Cx43 puncta discernibly (Figure 11A, compare panels in the top row with the middle row). Moreover, these puncta neither colocalized with GM130 (Figure 11A, middle row) nor with calreticulin, an ER-resident protein (Caramelo and Parodi, 2008) (data not shown). We also found that treatment of RL-NΔE cells with monensin for 2–4 h blocked the transport of Cx43 in the *cis*-Golgi, as assessed by its extensive colocalization with GM130 in the perinuclear regions, but did not appear to diminish the number of intracellular puncta. Moreover, these puncta still persisted when brefeldin and monensin treated RL-NΔE cells were extracted in situ with 1% TX-100 although the perinuclear staining specific for Cx43 and GM130 was lost (data not shown).

Intriguingly, treatment of RL-EΔN cells with brefeldin for 1–4 h also fragmented Golgi, but, in contrast to N-Cad expressing RL-NΔE cells, seemed to enhance GJ assembly or stabilize GJ plaques as assessed visually by the appearance of larger puncta at areas of cell–cell contact. As has been observed by others, in untreated RL-EΔN cells, Cx43 appeared to colocalize with GM130 near the perinuclear regions (Figure 11B, top row). Also, treatment of RL-EΔN cells with monensin not only caused accumulation of Cx43 in perinuclear regions, as assessed by its extensive colocalization with GM130 but also appeared to increase the number of intracellular puncta in some cells, which possibly represent endocytosed or degraded GJs (Figure 11B, compare panels in to top row with the bottom row). We also found that when RL-EΔN cells were treated with brefeldin and monensin for more than 4 h GJ assembly was drastically disrupted, with concomitant increase in the number of intracellular puncta (data not shown). Taken together, the data shown in Figures 10 and 11, combined with those shown in Figures 4, 8, and 9, suggest that detergent resistant intracellular puncta in N-Cad expressing RL-NΔE cells are likely generated at the site of cell–cell contact—and not en route from ER to cell surface via Golgi and trans-Golgi network—and possibly represent minuscule annular GJs, which become detergent-insoluble and eventually degrade in the lysosomes. The data obtained from single cells suggest that undocked connexons in both RL-NΔE and RL-EΔN cells most likely are endocytosed by both a clathrin-dependent and nonclathrin-dependent pathway.

Cadherin Expression and Assembly of Cx32 into Gap Junctions in RL-EΔN and RL-NΔE Cells

To investigate whether the assembly of other Cxs into GJs was also regulated differentially by E- and N-Cad, we introduced rat Cx32 into RL-EΔN and RL-NΔE cells, which do not express this Cx, by recombinant retroviruses and examined its subcellular fate in pooled polyclonal cultures within 2–3 passages after selection in G418. We chose Cx32 because it is expressed only by well-differentiated and polarized cells (Bavamian *et al*., 2009). We found that Cx32 was assembled efficiently into GJs in RL-EΔN cells but not in RL-NΔE cells where it remained intracellular as discrete puncta that also remained detergent-insoluble as assessed immunocytochemically upon in situ extraction with 1% TX-100 (Figure 12A) and biochemically by the detergent insolubility assay (Figure 12B) similar to what was observed with Cx43. Moreover, we found that both junctional and nonjunctional Cx43 and Cx32 did not appear to colocalize significantly in RL-EΔN and RL-NΔE cells. Taken together, these data suggest that N-Cad expression also prevents the assembly of Cx32 into GJs, possibly by triggering its endocytosis into detergent-insoluble puncta.

Cadherin Expression and Gap Junction Assembly in Mouse Mammary Tumor Cell Line

To assess the relevance of our findings in RL-CL9 cells further, we examined whether E-Cad and N-Cad expression also regulated the assembly of Cx43 into GJs differentially in other cell culture model systems, such as in the mouse mammary epithelial cell line (NMuMG), which has been widely used to study EMT (Maeda *et al*., 2005). These cells express E-Cad and N-Cad and undergo EMT in response to transforming growth factor β (Maeda *et al*., 2005). We found that in parental NMuMG cells that expressed nearly equal levels of both E-Cad and N-Cad, Cx43 was localized both at areas of cell–cell contact and in the cytosol (Figure S-6, top row). In a subclone of NMuMG that expressed a higher level of E-Cad compared with N-Cad (clone E9), Cx43 was predominantly assembled into GJs (Figure S-6, middle row), whereas in a clone that expressed only N-Cad and undetectable levels of E-Cad (clone 11), Cx43 remained intracellular just like in RL-NΔE cells (Figure S-6, bottom row). These data suggest that the expression of N-Cad also disrupts the assembly of Cx43 into GJs in NMuMG cells.

DISCUSSION

Our findings demonstrate that E-Cad and N-Cad have distinct effects on the assembly of Cx43 into GJs in isogenic subclones of RL-CL9 cells that express either one or the other cadherin. A key conclusion of our study is that Cx43 undergoes a profoundly different subcellular fate dependent on the type of cadherin expressed. When only E-Cad is expressed, Cx43 is preponderantly assembled into large GJs and when only N-Cad is expressed, Cx43 is endocytosed by a nonclathrin-mediated pathway before its assembly into functional GJs. Moreover, when both cadherins are simultaneously expressed in the same cell type, GJ assembly and disassembly seemed to occur concurrently. This conclusion is based on the screening of 60–92 isogenic E-Cad and N-Cad expressing clones and performing a systematic analysis of junctional and nonjunctional fate of Cx43 in selected clones. This analysis showed that intracellular localization of Cx43 as discrete vesicular puncta always coincided with the cell surface expression of N-Cad, whereas junctional localization coincided with the cell surface expression of E-Cad.

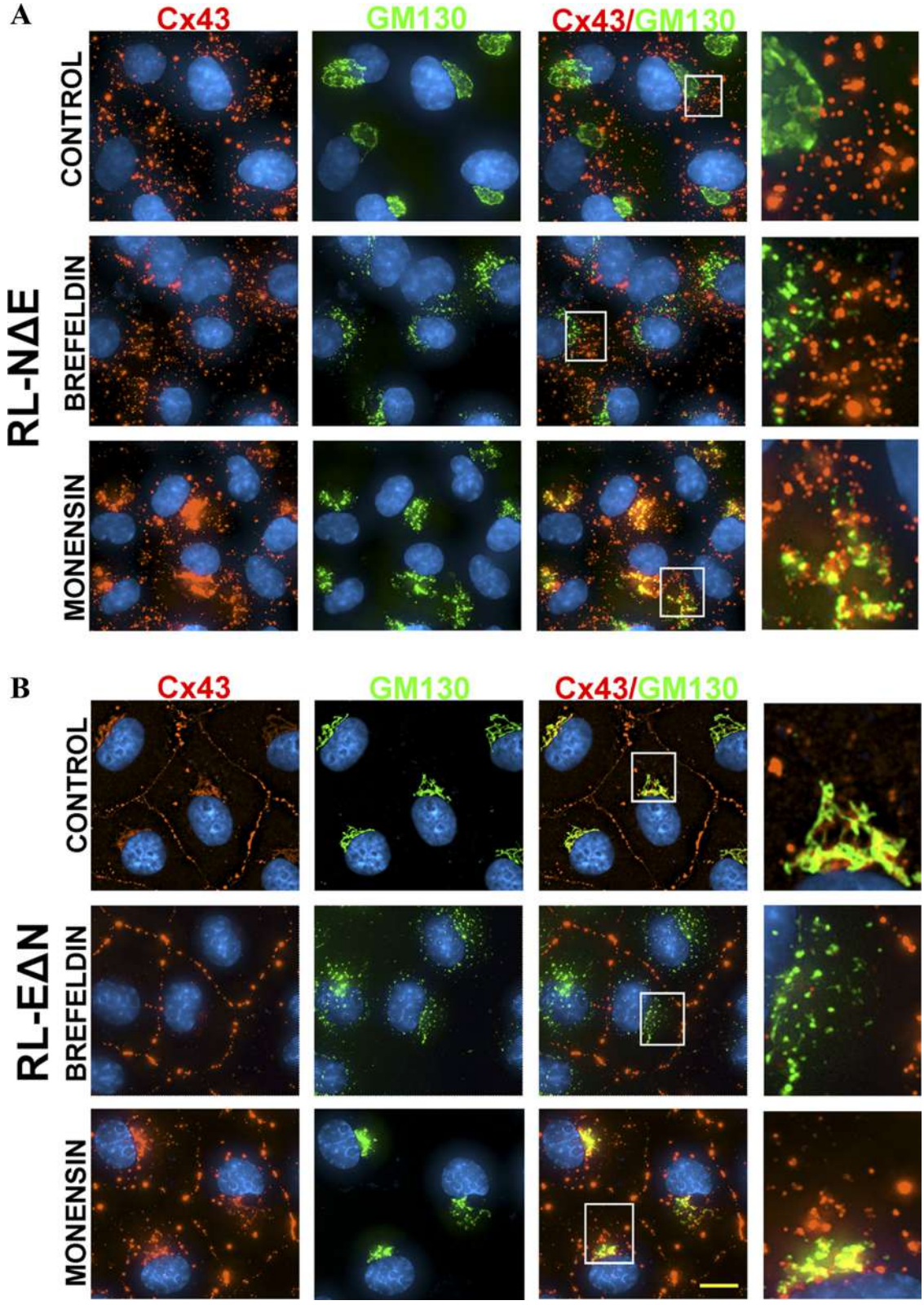

Figure 11. Detergent-resistant intracellular puncta are not generated along the secretory pathway in RL-NΔE cells. RL-NΔE (A) and RL-EΔN (B) cells were seeded in 6-cm Petri dishes and allowed to attain confluence. Cells were treated with brefeldin or monensin (10 μM) for 2 h and immunostained for Cx43 and GM130, a *cis*-Golgi resident protein (see Materials and Methods). Enlarged images marked by the white boxes are shown on the right. Note that both in RL-NΔE cells (A) and RL-EΔN cells (B), brefeldin disrupted the Golgi. Note also that brefeldin did not decrease the number of Cx43 puncta in RL-NΔE (A) cells but seemed to have stabilized or increase GJ plaques in RL-EΔN cells (B). Note a significant colocalization of Cx43 with GM130 due to the blockade of intraGolgi transport by monensin. Note also that monensin did not decrease the number of Cx43 puncta in RL-NΔE cells. Bar = 8 μm.

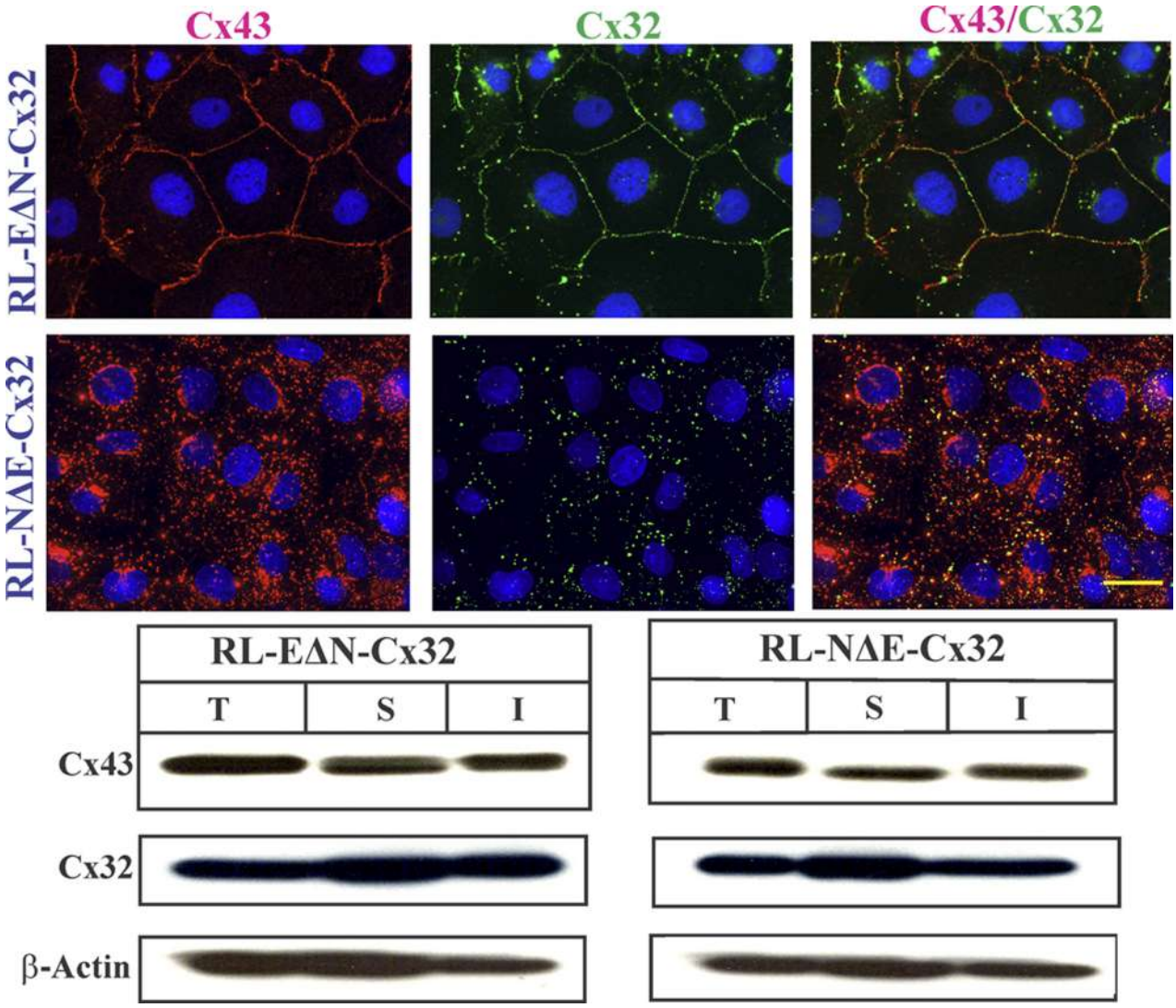

Figure 12. Differential assembly of Cx32 in RL-EΔN and RL-NΔE cells. (A) RL-EΔN and RL-NΔE cells were infected with recombinant retrovirus harboring rat Cx32 and pooled polyclonal cultures were immunostained for Cx43 and Cx32 after in situ extraction with 1% TX-100. Note that both Cxs assemble into GJs in RL-EΔN cells but remain intracellular in RL-NΔE cells. (B) Cell lysates prepared from pooled polyclonal cultures were analyzed by the detergent-solubility assay. Total (T), TX-100-soluble (S), and TX–insoluble (I) fractions were analyzed by Western blot analysis as described in Materials and Methods. The blots were stripped and reprobed with anti–β-actin antibody to verify equal loading. Note that both Cx43 and Cx32 are detected in detergent-soluble and detergent-insoluble fractions in both cell types. Bar = 20 μm.

Thus, through the dissection of the relative contributions of E-Cad and N-Cad, we have discovered a distinct role of each cadherin in regulating the assembly of Cx43 into GJs in RL-CL9 cells. Our studies show that GJ assembly and disassembly are the down-stream targets of the signaling initiated by E-Cad and N-Cad, respectively, and may provide one possible explanation for the disparate role played by these cadherins in regulating cell motility and invasion during tumor progression and EMT.

Our biotinylation data showed that intracellular accumulation of Cx43 was not caused by impaired trafficking because Cx43 trafficked normally to the cell surface and was degraded with similar kinetics in both RL-EΔN and RL-NΔE cells (Figure 7). However, GJ assembly was attenuated only in cells that expressed N-Cad and was recuperated only in those cells in which the expression of N-Cad was knocked down (Figure 5). Moreover, our biochemical and immunocytochemical data showed that a significant proportion of Cx43 remained detergent-insoluble both in RL-EΔN and RL-NΔE cells despite the fact that no functional GJs were assembled in the latter (Figures 3 and 4). These findings were intriguing because acquisition of detergent insolubility had been generally attributed to the incorporation of Cxs into GJs—and not to their intracellular and nonjunctional localization (VanSlyke and Musil, 2000; Musil, 2009). On the basis of these findings, we rationalized that the detergent-resistant intracellular vesicular puncta in N-Cad expressing RL-NΔE cells arose because of endocytosis of Cx43 in a nonclathrin-dependent manner. This notion was corroborated by our subsequent data, which showed that inhibition of clathrin-independent endocytosis by filipin and MβCD, which disrupt lipid rafts and endocytosis mediated by them, not only caused the disappearance of these intracellular puncta but also restored GJ formation robustly in N-Cad expressing RL-NΔE cells, confirming the requirement for the productive endocytosis in the generation of detergent-resis-

tant vesicular puncta and its inhibition for the formation of GJs. The lack of colocalization of these detergent-resistant intracellular Cx43 containing vesicular puncta with EEA-1, Rab5, caveolin-1, caveolin-2 suggests that Cx43 in RL-NΔE cells is endocytosed in a Rab5-independent manner into Rab5-negative vesicles that mature into Rab7-positive late endosomes, which are then targeted to the lysosomes for degradation (Figures 9 and S-5).

Because the kinetics of degradation of cell-surface associated Cx43 was not appreciably different in RL-EΔN and RL-NΔE cells (Figure 7), we rationalized that the detergent-resistant intracellular puncta in the latter arose at areas of cell–cell contact upon arrival of Cx43 (connexons) at the cell surface—and not en route to the cell surface along the secretory pathway. The lack of colocalization of these detergent-resistant intracellular Cx43 containing vesicles with conventional early endocytic markers further raised the possibility that the puncta did not arise by a canonical endocytic route and thus might be minuscule annular GJs which were endocytosed before maturing into larger functional GJ plaques and which incidentally became detergent-insoluble. Minuscule annular GJs of <0.5 μm have been observed in earlier studies (Jordan *et al*., 2001; Baker *et al*., 2008) and smaller GJ plaques have also been found to be extremely unstable (Holm *et al*., 1999; Jordan *et al*., 1999). The notion that detergent-resistant intracellular vesicular puncta arose at cell–cell contacts was substantiated by our experimental data with single cells, which showed that Cx43 puncta, both intracellular as well as at the cell peripheries, colocalized with clathrin, EEA-1, and Cav-1 and remained detergent soluble (Figure 10 and data not shown). Moreover, inhibition of ER to Golgi transport with brefeldin and inhibition of Golgi to cell surface transport with monensin had no discernible effect on the number of intracellular puncta in RL-NΔE cells (Figure 11A), which suggests that the intracellular puncta are not generated along the secretory pathway due to impaired trafficking but arise at sites of cell–cell contact upon arrival of Cx43 at the cell surface. TX-100 insoluble immunofluorescent E-Cad puncta, barely resolvable by standard microscopy, have been observed during the early stages of adherens junction formation at sites of cell–cell contact before they coalesce to form larger plaques (Yonemura *et al*., 1995; Adams *et al*., 1996). Although it is at present unclear at what stage of maturation a GJ plaque becomes detergent-insoluble, and in general what is the molecular basis of acquisition of detergent-insolubility by macromolecular complexes, it seems likely that the expression of N-Cad triggers the formation of these detergent-resistant intracellular puncta in RL-NΔE by preventing the coalescence of minuscule GJs, and triggering their endocytosis by a non-clathrin-dependent pathway before they form large GJs.

E-Cad is predominantly expressed in epithelial cells whereas N-Cad is expressed in neuronal and mesenchymal cells (Tepass *et al*., 2000; Gumbiner, 2005), and both cadherins have been shown to facilitate the assembly of Cx43 into GJs (Wei *et al*., 2005; Li *et al*., 2008; Chakraborty *et al*., 2010). It is of note that N-Cad is the main cadherin expressed in cardiac myocytes where it is required for the assembly of Cx43 into GJs (Li *et al*., 2005; Li *et al*., 2008). Although cell–cell adhesion mediated by cadherins has been shown to control the assembly of several junctional complexes, including GJs, it is as yet unknown how they signal (Gumbiner, 2005; Nelson, 2008; Wheelock *et al*., 2008; Sepniak *et al*., 2009). As assessed by cell–cell aggregation assays, our results showed that cell–cell adhesion mediated by both E-Cad and N-Cad remained intact in RL-EΔN and RL-NΔE cells (Table S-2). Thus, attenuation of junction formation in N-Cad expressing cells was not the result of absent cell–cell adhesion, although our data do not exclude the possibility that the distinct effects were caused by the quantitative and qualitative difference in the strength of cell–cell adhesion mediated by these cadherins. Our data also showed that GJ assembly was partially restored in N-Cad expressing RL-NΔE cells upon expression of E-Cad and was partially disrupted upon expression of N-Cad in E-Cad expressing RL-EΔN cells. Thus, when both cadherins were expressed simultaneously in the same cell, both assembly and disassembly seemed to occur concurrently.

What might be the possible molecular explanation for the diametrically opposite effects of E-Cad and N-Cad on the assembly of Cx43 into GJs in these cells? One plausible explanation for these data is that engagement of E-Cad and N-Cad triggers distinct signaling pathways, or recruits a distinct set of proteins to sites of cell–cell contact, or both, which affect GJ assembly differently. N-Cad, which is normally expressed in mesenchymal cells, has been shown to facilitate or enhance fibroblast growth factor receptor mediated signaling by preventing ligand-induced internalization of the receptor and through activation of sustained MAPK-ERK signaling cascade when expressed in tumor cells of epithelial origin (Hazan *et al*., 2000; Suyama *et al*., 2002; Hulit *et al*., 2007). Similarly, E-Cad has also been shown to interact or associate with receptors for fibroblast growth factor and epidermal growth factor, leading to the attenuation of signaling as well as to modulation of MAPK-ERK signaling cascade (Pece *et al*., 1999; Pece and Gutkind, 2000; Perrais *et al*., 2007). Thus, E-Cad and N-Cad engagement may have several distinct downstream molecular targets that might facilitate or attenuate GJ assembly differently independent of cell–cell adhesion and dependent upon the signaling pathway initiated upon expression. As Cx43 has been shown to be endocytosed in response to growth factors, such as epidermal growth factor, this may be one possible explanation for the disparate effect of E-Cad and N-Cad on GJ assembly in RL-EΔN and RL-NΔE cells. Further studies using the constitutively active mutants of epidermal growth factor receptor as well as knock down studies with fibroblast growth factor receptors will be required to substantiate this notion.

As GJ assembly and disassembly occurred concurrently when both cadherins were simultaneously expressed in the same cell type, it is also possible that the assembly of Cx43 is independently regulated by E-Cad and N-Cad, locally, through recruitment of separate sets of proteins to the site of cell–cell contact or through their segregation into distinct membrane microdomains, which determines junctional versus nonjunctional fate of Cx43 upon arrival at the cell surface. This explanation is in accord with the findings that Cxs lie in the vicinity of cadherins and their associated proteins α- and β-catenins during GJ assembly and disassembly and may also associate with them transiently either directly or indirectly (Fujimoto *et al*., 1997; Wei *et al*., 2005; Xu *et al*., 2006). In mesenchyme-derived NIH3T3 cells, which express N-Cad, interaction between Cx43 and N-Cad was required for GJ assembly and turnover at the cell surface (Wei *et al*., 2005). Moreover, when coexpressed in the same cells, E-Cad and N-Cad are likely to exist in separate complexes as their interaction is not heterophilic (Tepass *et al*., 2000; Gumbiner, 2005). Furthermore, N-Cad and Cxs have been found to be concentrated in lipid rafts and interaction between N-Cad and p120 catenin, which also interacts with Cx43 (Wei *et al*., 2005), occurs in cholesterol-rich environment (Locke *et al*., 2005; Taulet *et al*., 2009). Finally, it is also possible that the expression of N-Cad could squelch away components which

otherwise would have been used by E-Cad to form mature adherens junctions to facilitate assembly. Because knockdown of N-Cad in RL-NΔE cells, which lack detectable level of E-Cad, restored GJ assembly, it is likely that other mechanisms, which are not mediated by these classical cadherins, or are induced upon knock down of cadherins, exist to restore and regulate the assembly of GJs. One possible mechanism is that cell–cell adhesion generated by the docking of connexons by themselves is sufficient to induce assembly in the absence of classical cadherins and it is utilized only when no other mechanism is active. This notion is corroborated by our recent studies, which showed that the assembly of Cx43 was induced in the absence of E-Cad mediated cell–cell adhesion in cadherin null human squamous carcinoma cells (Chakraborty *et al*., 2010) and by other studies in which expression of Cx43 induced cell–cell adhesion of its own (Lin *et al*., 2002; Cotrina *et al*., 2009).

While the molecular mechanism(s) by which E-Cad and N-Cad affect the assembly of Cx43 into GJs in an opposite manner remains to be elucidated, regulation of endocytosis of minuscule GJ puncta at the areas of cell–cell contact before they mature into larger plaques seems to be the determining factor that dictates the assembly of GJs in RL-CL9 cells. Alternatively, because raft component proteins are expected to have decreased lateral mobility (Lingwood and Simons, 2010), attenuation of junction assembly may result from the decreased lateral mobility of docked connexons due to their entrapment in lipid rafts. This notion is in agreement with our data, which showed that the stability of cell-surface associated Cx43 remained unaffected, although it remains to be seen whether the surface residence time of connexons was also significantly reduced, which either prevented their recruitment to nascent minuscule GJ plaques or permitted their endocytosis before docking in N-Cad expressing RL-NΔE cells compared with E-Cad expressing RL-EΔN cells. Because the assembly of Cx32 into GJs was also regulated in diametrically opposed ways in RL-EΔN and RL-NΔE cells, it appears that the effect of N-Cad expression on junction assembly is not Cx specific. Hence, expression of N-Cad in epithelial cells, which normally do not express it, creates a milieu at the areas of cell–cell contact that is nonconducive for the assembly of larger GJ plaques. Moreover, the findings that the assembly of Cx43 into GJs appeared to be similarly affected in the mouse mammary epithelial cell line, NuMuG, which is widely used for studying EMT (Maeda *et al*., 2005), suggests that the differential effect of E-Cad and N-Cad in regulating GJ assembly and disassembly may be a general feature of tumor epithelial cells that express both cadherins.

What might be the physiological significance of these findings? E-Cad and N-Cad have been shown to play opposite role in controlling cell migration, motility, and invasion of tumor cells in vitro and in vivo (Cavallaro and Christofori, 2004; Thiery *et al*., 2009). Also, a switch in N-Cad expression with or without concomitant loss of E-Cad expression—commonly referred to as cadherin switching—is often observed in cells during EMT and during the progression of carcinomas from an indolent state to a more invasive state (Wheelock *et al*., 2008). N-Cad has been found to be at the invasive front of several tumors (Cavallaro and Christofori, 2004) and the expression of Cx43 in some tumor cell lines has also been associated with the acquisition of invasive potential (Olk *et al*., 2009). Recent studies showed that knock down of Cx43 disrupted cell–cell adhesion, reduced cell polarity and focal adhesion plaques, but increased speed of migration and cell protrusive activity in cells derived from epicardium and in neural crest cells that express N-Cad (Xu *et al*., 2006; Rhee *et al*., 2009). Disruption of several junctional complexes is a hallmark of tumor progression and invasion as well as of EMT(Mosesson *et al*., 2008; Thiery *et al*., 2009). Tumor cells have now been shown to migrate and invade both as single cells and collectively (Friedl and Gilmour, 2009). Moreover, endocytosis has emerged as an important process that orchestrates cell motility and migration by regulating the spatial distribution of signaling molecules, such as cell surface receptors and their downstream effectors (Lanzetti and Di Fiore, 2008; Sorkin and von Zastrow, 2009). In the light of these studies, it is tempting to speculate that bidirectional signaling between Cxs and cadherins in normal and tumor cells is fine-tuned to control the assembly of GJs as well as other junctional complexes to modulate the polarized and differentiated state and to modulate cell motility and invasion under normal and pathological states.

ACKNOWLEDGMENTS

We thank Linda Kelsey for her expert technical help. We thank Tom Dao for help with live cell imaging. We thank Drs. S. Caplan and Naava Naslavsky for helpful suggestions and discussion throughout the course of this study. This research was supported by National Institutes of Health Grant CA113903, Department of Defense Prostate Cancer Research Program Grant 081198, and Nebraska State Grant LB506 (to P.P.M.) and RO-1DE12308 (to K.R.J.). We gratefully acknowledge support from the Nebraska Center for Cellular Signaling and Cancer Graduate Research Training Program of Eppley Institute in the form of fellowships (to S.C. and K.E.J., respectively).

REFERENCES

Adams, C., Nelson, J. W., and Smith, S. J. (1996). Quantitative analysis of cadherin-catenin-actin reorganization during development of cell-cell adhesion. J. Cell Biol. *135*, 1899–1911.

Baker, S. M., Kim, N., Gundersen, G. G., Segretain, D., and Falk, M. M. (2008). Acute internalization of gap junctions in vascular endothelial cells in response to inflammatory mediator-induced G-protein coupled receptor activation. FEBS Letters *582*, 4039–4046.

Bavamian, S., Klee, P., Allagnat, F., Haefliger J.-A., and Meda, P. (2009). Connexins and Secretion. In: Connexins: A Guide, ed. A. Harris and D. Locke Springer, 511–528.

Bryant, D. M., and Mostov, K. E. (2008). From cells to organs: building polarized tissue. Nat. Rev. Mol. Cell Biol. *9*, 887–901.

Caramelo, J. J., and Parodi, A. J. (2008). Getting in and out from calnexin/calreticulin cycles. J. Biol. Chem. *283*, 10221–10225.

Cavallaro, U., and Christofori, G. (2004). Cell adhesion and signalling by cadherins and Ig-CAMs in cancer. Nat. Rev. Cancer *4*, 118–132.

Chakraborty, S., Mitra, S., Falk, M. M., Caplan, S., Wheelock, M. J., Johnson, K. R., and Mehta, P. P. (2010). E-cadherin differentially regulates the assembly of connexin43 and connexin32 into gap junctions in human squamous carcinoma cells. J. Biol. Chem. *285*, 10761–10776.

Chardin, P., and McCormick, F. (1999). Brefeldin A: the advantage of being uncompetitive. Cell *97*, 153–155.

Cotrina, M. L., Lin, J. H., and Nedergaard, M. (2009). Adhesive properties of connexin hemichannels. Glia *56*, 1791–1798.

Crespin, S., Defamie, N., Cronier, L., and Mesnil, M. (2009). Connexins and carcinogenesis. In: Connexinss: A Guide, ed. A. Harris and D. Locke 529–542.

Falk, M. M., Baker, S. M., Gumpert, A., Segretain, D., and Buckheit, R. W. (2009). Gap junction turnover is achieved by the internalization of small endocytic double-membrane vesicles. Mol. Biol. Cell *20*, 3342–3352.

Friedl, P., and Gilmour, D. (2009). Collective cell migration in morphogenesis, regeneration and cancer. Nat. Rev. Mol. Cell Biol. *10*, 445–457.

Fujimoto, K., Nagafuchi, A., Tsukita, S., Kuraoka, A., Ohokuma, A., and Shibata, Y. (1997). Dynamics of connexins, E-cadherin and a- catenin on cell membranes during gap junction formation. J. Cell Sci. *110*, 311–322.

Goodenough, D. A., and Paul, D. L. (2009). Gap junctions. Cold Spring Harb. Perspect. Biol. *1*, a002576

Govindarajan, R., Song, X.-H., Guo, R.-J., Wheelock, M. J., Johnson, K. R., and Mehta, P. P. (2002). Impaired traffcking of connexins in androgen-independent human prostate cancer cell lines and its mitigation by a-catenin. J. Biol. Chem. *277*, 50087–50097.

Gumbiner, B. M. (2005). Regulation of cadherin-mediated adhesion and morphogenesis. Nat. Rev. Mol. Cell Biol. *6*, 622–634.

Hazan, R. B., Phillips, G. R., Qiao, R. F., and Norton, L. (2000). Exogenous expression of N-cadherin in breast cancer cells induces cell migration, invasion, and metastasis. J. Cell Biol. *148*, 779–790.

Hernandez-Blazquez, F., Joazeiro, P., Omori, Y., and Yamasaki, H. (2001). Control of intracellular movement of connexins by E-cadherin in murine skin papilloma cells. Exp. Cell Res. *270*, 235–247.

Heuser, J. E., and Anderson, R. G. (1989). Hypertonic media inhibit receptor-mediated endocytosis by blocking clathrin-coated pit formation. J. Cell Biol. *108*, 389–400.

Holm, I., Mikhailov, A., Jilson, T., and Rose, B. (1999). Dynamics of gap junctions observed in living cells with connexin43-GFP chimeric protein. Euro J. Cell Biol. *78*, 856–866.

Hulit, J., *et al.* (2007). N-cadherin signaling potentiates mammary tumor metastasis via enhanced extracellular signal-regulated kinase activation. Cancer Res. *67*, 3106–3116.

Jongen, W., Fitzgerald, D., Asamoto, M., Piccoli, C., Slaga, T., Gros, D., Takeichi, M., and Yamasaki, H. (1991). Regulation of connexin 43-mediated gap junctional intercellular communication by Ca^{2+} in mouse epridermal cells is controlled by E-cadherin. J. Cell Biol. *114*, 545–555.

Jordan, K., Solan, J. L., Dominguez, M., Sia, M. A., Hand, A., Lampe, P. D., and Laird, D. W. (1999). Trafficking, assembly, and function of a connexin43-green fluorescent protein chimera in live mmamalian cells. Mol. Biol. Cell *10*, 2033–2050.

Jordan, K., Chodock, R., Hand, A., and Laird, D. W. (2001). The origin of annular junctions: a mechanism of gap junction internalization. J. Cell Sci. *114*, 763–773.

Kim, J.-B., Islam, S., Kim, Y. J., Prudoff, R. S., Sass, K. M., Wheelock, M. J., and Johnson, K. R. (2000a). N-cadherin extracellular repeat 4 mediates epithelial to mesenchymal transition and increased motility. J. Cell Biol. *151*, 1193–1205.

Kim, S. H., Li, Z., and Sacks, D. B. (2000b). E-cadherin-mediated cell-cell attachment activates Cdc42. J. Biol. Chem. *275*, 36999–37005.

King, T. J., and Lampe, P. D. (2004). The gap junction protein connexin32 is a mouse lung tumor suppressor. Cancer Res. *64*, 7191–7196.

Klausner, R. D., Donaldson, J. G., and Lippincott-Schwartz, J. (1992). Brefeldin A: Insights into the control of membrane traffic and organelle structure. J. Cell Biol. *116*, 1071–1080.

Kojima, T., Murata, M., Go, M., Spray, D. C., and Sawada, N. (2007). Connexins induce and maintain tight junctions in epithelial cells. J. Membr. Biol. *217*, 13–19.

Laird, D. W. (2006). Life cycle of connexins in health and disease. Biochem. J. *394*, 527–543.

Laird, D. W. (2010). The gap junction proteome and its relationship to disease. Trends Cell Biol. *20*, 92–101.

Langlois, S., Cowan, K. N., Shao, Q., Cowan, B. J., and Laird, D. W. (2008). Caveolin-1 and -2 interact with connexin43 and regulate gap junctional intercellular communication in keratinocytes. Mol. Biol. Cell *19*, 912–928.

Lanzetti, L., and Di Fiore, P. (2008). Endocytois and cancer : an "insider" network with dangerous liaisons. Traffic *9*, 2011–2021.

Li, J., Levin, M. D., Xiong, Y., Petrenko, N., Patel, V. V., and Radice, G. L. (2008). N-cadherin haploinsufficiency affects cardiac gap junctions and arrhythmic susceptibility. J. Mol. Cell Cardiol. *44*, 597–606.

Li, J., Patel, V. V., Kostetskii, I., Xiong, Y., Chu, A. F., Jacobson, J. T., Yu, C., Morley, G. E., Molkentin, J. D., and Radice, G. L. (2005). Cardiac-specific loss of N-cadherin leads to alteration in connexins with conduction slowing and arrhythmogenesis. Circ. Res. *97*, 474–481.

Lin, J. H., *et al.* (2002). Connexin 43 enhances the adhesivity and mediates the invasion of malignant glioma cells. J. Neurosci. *22*, 4302–4311.

Lingwood, D., and Simons, K. (2010). Lipid rafts as a membrane-organizing principle. Science *327*, 46–50.

Locke, D., Liu, J., and Harris, A. L. (2005). Lipid rafts prepared by different methods contain different connexin channels, but gap junctions are not lipid rafts. Biochemistry *44*, 13027–13042.

Maeda, M., Johnson, K. R., and Wheelock, M. J. (2005). Cadherin switching: essential for behavioral but not morphological changes during an epithelium-to-mesenchyme transition. J. Cell Sci. *118*, 873–887.

Maeda, M., Shintani, Y., Wheelock, M. J., and Johnson, K. R. (2006). Src activation is Not necessary for transforming growth factor (TGF)-{beta}-mediated epithelial to mesenchymal transitions (EMT) in mammary epithelial cells: PP1 directly inhibits TGF-{beta} receptors I and II. J. Biol. Chem. *281*, 59–68.

Marra, P., Salvatore, L., Mironov, A., Jr., Di Campli, A., Di Tullio, G., Trucco, A., Beznoussenko, G., Mironov, A., and De Matteis, M. A. (2007). The biogenesis of the Golgi ribbon: the roles of membrane input from the ER and of GM130. Mol. Biol. Cell *18*, 1595–1608.

McLachlan, E., Shao, Q., Wang, H. L., Langlois, S., and Laird, D. W. (2006). Connexisn act as tumor suppressors in three dimensional mammary cell organoids by regulating differentiation and angiogenesis. Cancer Res. *66*, 9886–9894.

Mehta, P. P., Perez-Stable, C., Nadji, M., Mian, M., Asotra, K., and Roos, B. (1999). Suppression of human prostate cancer cell growth by forced expression of connexin genes. Dev. Genetics *24*, 91–110.

Mehta, P. P., Yamamoto, M., and Rose, B. (1992). Transcription of the gene for the gap junctional protein connexin43 and expression of functional cell-to-cell channels are regulated by cAMP. Mol. Biol. Cell *3*, 839–850.

Mehta, P., Bertram, J., and Loewenstein, W. (1986). Growth inhibition of transformed cells correlates with their junctional communication with normal cells. Cell *44*, 187–196.

Meyer, R., Laird, D., Revel, J.-P., and Johnson, R. (1992). Inhibition of gap junction and adherens junction assembly by connexin and A-CAM antibodies. J. Cell Biol. *119*, 179–189.

Mitra, S., Annamali, L., Chakraborty, S., Johnson, K., and Mehta, P. P. (2006). Androgen-regulated formation and degradation of gap junctions in androgen-responsive human prostate cancer cells. Mol. Biol. Cell *17*, 5400–5417.

Mosesson, Y., Mills, G. B., and Yarden, Y. (2008). Derailed endocytosis: an emerging feature of cancer. Nat. Rev. Cancer *8*, 835–850.

Musil, L. S. (2009). Biogenesis and degradation of gap junctions. In: Connexins: A Guide, ed. A. Harris and D. Locke Springer, 225–240.

Musil, L., Cunningham, B. A., Edelman, G., and Goodenough, D. (1990). Differential phosphorylation of the gap junction protein connexin43 in junctional communicaton-competent and -deficient cell lines. J. Cell Biol. *111*, 2077–2088.

Nelson, W. J. (2008). Regulation of cell-to-cell adhesion by the cadherin-a-catenin complex. Biochem. Soc. Trans. *36*, 149–155.

Nieman, M. T., Kim, J.-B., Johnson, K. R., and Wheelock, M. J. (1999). Mechanism of extracellular domain-deleted dominant negative cadherins. J. Cell Sci. *112*, 1621–1632.

Olk, S., Zoidl, G., and Dermietzel, R. (2009). Connexins, cell motility, and the cytoskeleton. Cell Motil. Cytoskeleton *66*, 1–17.

Orlandi, P. A., and Fishman, P. H. (1998). Filipin-dependent inhibition of cholera toxin: evidence for toxin internalization and activation through caveolae-like domains. J. Cell Biol. *141*, 905–915.

Pece, S., Chiariello, M., Murga, C., and Gutkind, J. S. (1999). Activation of the protein kinase Akt/PKB by the formation of E-cadherin-mediated cell-cell junctions. J. Biol. Chem. *274*, 19347–19351.

Pece, S., and Gutkind, J. S. (2000). Signaling from E-cadherins to the MAPK pathway by the recruitment and activation of epidermal growth factor receptors upon cell-cell contact formation. J. Biol. Chem. *275*, 41227–41233.

Perrais, M., Chen, X., Perez-Moreno, M., and Gumbiner, B. M. (2007). E-cadherin homophilic ligation inhibits cell growth and epidermal growth factor receptor signaling independently of other cell interactions. Mol. Biol. Cell *18*, 2013–2025.

Piehl, M., Lehmann, C., Gumpert, A., Denizot, J. P., Segretain, D., and Falk, M. M. (2007). Internalization of large double-membrane intercellular vesicles by a clathrin-dependent endocytic process. Mol. Biol. Cell *18*, 337–347.

Rhee, D. Y., Zhao, X. Q., Francis, R.J.B., Huang, G. Y., Mably, J. D., and Lo, C. W. (2009). Connexin 43 regulates epicardial cell polarity and migration in coronary vascular development. Development *136*, 3185–3193.

Rohrer, J., Schweizer, A., Russell, D., and Kornfeld, S. (1996). The targeting of Lamp1 to lysosomes is dependent on the spacing of its cytoplasmic tail tyrosine sorting motif relative to the membrane. J. Cell Biol. *132*, 565–576.

Saez, J. C., Berthoud, V. M., Branes, M. C., artinez, A. D., Bey., and Beyer, E. C. (2003). Plasma membrane channels formed by connexins: their regulation and functions. Physiol. Rev. *83*, 1359–1400.

Segretain, D., and Falk, M. M. (2004). Regulation of connexin biosynthesis, assembly, gap junction formation, and removal. Biochim. Biophys. Acta *1662*, 3–21.

Sepniak, E., Radice, G. L., and Vasioukhin, V. (2009). Adhesive and signaling functions of cadherins and catenins in vertebrate development. Cold Spring Harb. Perspect. Biol. *1*, 1–13.

Shintani, Y., Fukumoto, Y., Chaika, N., Svoboda, R., Wheelock, M. J., and Johnson, K. R. (2008). Collagen I-mediated up-regulation of N-cadherin requires cooperative signals from integrins and discoidin domain receptor 1. J. Cell Biol. *180*, 1277–1289.

Skretting, G., Torgersen, M. L., van Deurs, B., and Sandvig, K. (1999). Endocytic mechanisms responsible for uptake of GPI-linked diphtheria toxin receptor. J. Cell Sci. *112*, 3899–3909.

Sorkin, A., and von Zastrow, M. (2009). Endocytosis and signalling: intertwining molecular networks. Nat. Rev. Mol. Cell Biol. *10*, 609–622.

Subtil, A., Hemar, A., and Dautry-Varsat, A. (1994). Rapid endocytosis of interleukin 2 receptors when clathrin-coated pit endocytosis is inhibited. J. Cell Sci. *107*, 3461–3468.

Suyama, K., Shapiro, I., Guttman, M., and Hazan, R. B. (2002). A signaling pathway leading to metastasis is controlled by N-cadherin and the FGF receptor. Cancer Cell *2*, 301–314.

Tartakoff, A. (1983). Perturbation of vesicular traffic with the carboxylic ionophore monensin. Cell *32*, 1026–1028.

Taulet, N., Comunale, F., Favard, C., Charrasse, S., Bodin, S. p., and Gauthier-Rouvi+¿re, C.+. (2009). N-cadherin/p120 catenin association at cell-cell contacts occurs in cholesterol-rich membrane domains and is required for rhoA Activation and myogenesis. J. Biol. Chem. *284*, 23137–23145.

Tepass, U., Trunong, K., Godt, D., Ikura, M., and Peifer, M. (2000). Cadherins in embryonic and neural morphogenesis. Nature Rev. Cell Mol. Biol. *1*, 91–100.

Thiery, J. P., Acloque, H., Huang, R.Y.J., and Nieto, M. A. (2009). Epithelial-mesenchymal transitions in development and disease. Cell *139*, 871–890.

VanSlyke, J. K., and Musil, L. S. (2000). Analysis of connexin intracellular transport and assembly. Methods *20*, 156–164.

Wang, L. H., Rothberg, K. G., and Anderson, R. G. (1993). Mis-assembly of clathrin lattices on endosomes reveals a regulatory switch for coated pit formation. J. Cell Biol. *123*, 1107–1117.

Wang, Y., and Rose, B. (1997). An inhibition of gap-junctional communication by cadherins. J. Cell Sci. *110*, 301–309.

Wei, C. J., Francis, R., Xu, X., and Lo, C. W. (2005). Connexin43 associated with an N-cadherin-containing multiprotein complex is required for gap junction formation in NIH3T3 cells. J. Biol. Chem. *280*, 19925–19936.

Wei, C. J., Xu, X., and Lo, C. W. (2004). Connexins and cell signaling in development and disease. Ann. Rev. Cell Dev. Biol. *20*, 811–838.

Wheelock, M. J., Buck, C., Bechtol, K., and Damsky, C. (1987). Soluble 80 Kd fragment of cell-CAM 120/180 disrupts cell-cell adhesion. J. Cell. Biochem. *34*, 187–202.

Wheelock, M. J., and Johnson, K. R. (2003). Cadherins as modulators of cellular phenotype. Annu. Rev. Cell Dev. Biol. *19*, 207–235.

Wheelock, M. J., Shintani, Y., Maeda, M., Fukumoto, Y., and Johnson, K. R. (2008). Cadherin switching. J. Cell Sci. *121*, 727–735.

Xu, X., Francis, R., Wei, C. J., Linask, K. L., and Lo, C. W. (2006). Connexin 43-mediated modulation of polarized cell movement and the directional migration of cardiac neural crest cells. Development *133*, 3629–3639.

Yonemura, S., Itoh, M., Nagafuchi, A., and Tsukita, S. (1995). Cell-to-cell adherens junction formation and actin filament organization: similarities and differences between non-polarized fibroblasts and polarized epithelial cells. J. Cell Sci. *108*, 127–142.